Small Scale Energy Harvesting for Use with an Electronic Door Strike

by

Grant Cechmanek

A thesis
presented to the University of Waterloo
in fulfillment of the

thesis requirement for the degree of

Master of Applied Science

in

Mechanical and Mechatronics Engineering

Waterloo, Ontario, Canada, 2016

I hereby declare that I am the sole author of this thesis. This is a true copy of the thesis, including any required final revisions, as accepted by my examiners.

I understand that my thesis may be made electronically available to the public.

ABSTRACT

Smart or connected devices are becoming more and more prevalent in modern society. These devices typically consist of miniature sensors and actuators to automate and control common daily activities. The spread of these devices comes with the need to supply power to these devices. A first approach is often to include a battery to allow for remote operation. The immediate drawback to this approach is the eventual need to either replace or recharge this battery. A power generation system that both compact and portable is desired. Any such system which can operate by extracting ambient energy from the environment would see applications in many common devices ranging from common calculators, to industrial equipment health monitoring systems.

One common device that is experiencing the transition from a purely mechanical to smart device is the standard door lock. Keyless access is gaining prevalence in both office buildings and private residences as it allows for greater convenience and added security measures. These benefits come at the cost of electrical energy consumption, which is presently being primarily supplied through direct wire routing from the building's main grid. An electronic locking mechanism that is fully physically autonomous and energy independent would be advantageous.

In this work the application of energy harvesting methods as they relate to an electronic door strike, or E-strike, are investigated. Multiple different common ambient energy sources are identified and their expected power densities quantified. These range from 9 μW to 7W depending on the source. From these sources human action is identified as possessing the highest power density, and also being the most reliably available source. A system to model the energy flow through an E-strike is derived. This model accounts the maximum available energy, harvesting efficiency, required power draw, and storage capabilities.

An E-strike prototype is constructed and experiments are conducted to validate the proposed model. The proposed design provides and energy density of 4.25mJ/cm^3. The overarching goal is to identify under what operating conditions an E-strike will be able to operate indefinitely, without the need to add physical power lines or replace batteries. A single combined parameter, the Activation-per-input value is defined and identified as the key characteristic that determines which environments will be suitable for an energy harvesting E-strike. Results of these experiments demonstrate that an E-strike can operate indefinitely with an Activation-per-Input ratio of 0.1 or below.

ACKNOWLEDGEMENTS

I would like to thank my supervisor, Professor Soo Jeon for his guidance and advice throughout my time spent at the University of Waterloo. I have learned a great deal from my time in his lab and am grateful for the opportunities made open to me.

I would also like to thank Ryan and Khalid at Rutherford Controls, who supported this interesting project and provided invaluable feedback and advice throughout the course of research and development.

I would like to thank all my friends that I have made during my time spent in Waterloo. We've worked on many projects together and have no doubt grown as engineers because of them. Special thanks to Dan Connolly for his addiction to challenging math problems and the help and advice he has given me on how to investigate the proposed energy harvester.

DEDICATION

This work is dedicated to all of my friends, those in Ontario and abroad, who supported me during my time in Waterloo.

CONTENTS

LIST OF TABLES

LIST OF FIGURES

1. INTRODUCTION

1.1.MOTIVATION

More and more modern devices are being marketed as 'smart' technologies. This term is used broadly to refer to devices which have functionality beyond their primary purpose. This functionality often includes wireless communication, automatic sensing and measurement, or built-in timing systems to better accommodate people. Examples include phone recharging cables that automatically disconnect power once the battery is full [1], or a mixed drink measuring gage that wirelessly connects to a smart phone application [2], or a shoe insole that relays a pressure map of your feet to your phone during athletic performance [3]. These are just a few of the more novel smart devices and while the specifics of each vary, there are a few features that have become increasingly common.

Smart devices are:

- Electronic. They actively consume electricity as a power source
- Autonomous. Most devices operate untethered from a power source and rely on periodic battery recharging
- Wireless. Communication, typically with a smart phone, is often a core feature and requirement for many devices

These requirements place a burden on low power electronics and battery technologies as users do not want to recharge or replace batteries often and product designers do not want to limit their product capabilities based on the available stored energy. The continuously increasing functionality of smart devices is leading to larger and larger energy demands on small scale systems.

With the ever increasing number of electronic devices becoming available in our daily lives the issue of how to provide them with power becomes more and more prevalent. To date advances in battery technologies have not been able to keep pace, with cell energy densities increasing by an average of only 3% annually over the past 60 years [4]. With batteries being either ill-suited or unable to meet device requirements alternative power sources must be sought. The applicability of energy scavenging technologies is growing to match these demands as these methods offer an alternative power source for small scale electronics.

Large wireless sensor networks (WSNs) also stand to benefit substantially from harvesting methods. Also called sensor networks, or sensor and actuator networks, these are a distributed set of independent sensor nodes that are deployed over some environment to periodically measure some parameter and relay this measurement to a central terminal through the network. These WSNs are often used for machine health monitoring, structural health monitoring, patient and healthcare monitoring, or environmental and air pollution monitoring. They possess a number of common features which make them ideal candidates to applied energy harvesting technologies, which are: low power consumption, intermittent activation, near an available energy source, and remotely located or inaccessible. Often the measurement parameter can double as an ambient power source, increasing the likelihood that harvesting methods will be applicable.

1.2.APPLICATION

Access control is one specific area of interest that may benefit from harvesting methods. Many buildings, both commercial and public, require the use of controlled access points to limit which individuals have access to specific areas. Examples include large office buildings that support multiple company offices, or research organizations that must restrict access to private work areas. While this has been traditionally done with physical locks and keys this method has limitations and disadvantages. Physical keys can be duplicated with relative ease, and if lost or stolen all corresponding locks must be replaced to ensure security. Electronic access allows for immediate updating of permissions and the removal of key cards. This work focuses on the development of an energy scavenging door strike and methods to increase its operational lifespan. Different potential energy sources will be identified and evaluated based on their suitability. Key design parameters of the door strike will be identified. Hybrid battery & harvesting designs will be investigated, and experimental results will be presented.

Currently, the largest drawbacks of electronic door locks are their power consumption requirements; typically necessitating a hard wiring into the building's main power grid. When this is done in modern building construction it may lead to running potentially hundreds, or even thousands of feet of electrical wire to every door, adding to the total system cost. In cases where existing buildings are renovated to include electronic locks there is often the additional cost of removing and reinstalling wall facades to enclose the power lines. A fully wireless, self-contained, device would have substantial market appeal.

A simple first approach could be the inclusion of a battery to each individual access point. The most apparent drawback of this potential solution is the occasional need to now replace these batteries. Feasibility of this approach will then depend on the frequency of replacement; once per day would be an unacceptable burden, whereas once per decade would be a nonissue. Quantified estimates of expected lifespan using only a battery are detailed in Section 3.4. Hybrid systems that utilize both a battery and harvesting technology in tandem may offer a suitable compromise between the two approaches, offering the reliability of a battery with the longevity of an energy harvester. Under the right conditions a harvester alone may be the optimal power supply. Determining under what circumstances a harvester outperforms a battery, and vice versa, is an important question that must be answered prior to implementing any device and a methodology to evaluate these tradeoffs is presented in Section 3.3.

1.3.OBJECTIVE

The objective of this work is to investigate the feasibility and applicability of energy harvesting technologies for an electronic door strike application. Several different harvesting techniques will be identified along with proposed modifications and enhancements to better suit incorporation into a door strike. Multiple different energy sources will be evaluated based on their maximum available power, availability, and reliability. From the investigation into different potential sources of energy a system that utilizes one or more of these sources will be developed and refined. Predictions of system performance will be compared to experimental data to verify a mathematical model of the energy flow through the door strike.

The ultimate goal is to develop a door strike with an effectively infinite operational lifespan. As will be shown in Section 3.4 the operational lifespan is heavily dependent on the environment in which the door strike is placed. As such, the key parameters impacting lifespan will be identified and their relative impact on performance will be quantified. This approach will allow individual environments to be characterized based on their suitability for the deployment of a harvesting strike.

1.4.RELATED WORK

Methods to extract energy from ambient sources have been studied at length by a number of researchers. This has led to a variety of different approaches with a wide range of performance. The optimal harvesting technique is often highly application specific as each situation will offer different power sources and have different power requirements.

One area where energy harvesting is seeing greater deployment is with wireless sensor networks (WSNs). These networks of autonomous devices are ideal candidates for harvesting technologies as they are typically low power, remotely located, and most importantly, almost always positioned near an available energy source. Quite often this source is itself the parameter which the sensor transducer is measuring (ex: mechanical vibrations, fluid flow rates, temperature gradients). Quantifying the different potential energy sources is then a first step in designing a harvesting system.

Catatore and Ouwerkerk [5] quantified the maximum available energy from a number of different practical sources including small machinery, automotive tires, and human gate. Comparing these sources to thermoelectric or photovoltaic sources the authors concluded that millimeter scale vibration harvesters can generate power levels exceeding 1mW, but this requires perfect matching between source and generator resonant frequency. This frequency matching must be done manually for each individual generator deployed and the process must be repeated if the source frequency changes. For systems where the source frequency constantly changes, such as automotive engines or wheel rotations, a generator may be tuned to the most commonly present frequency, at a cost of not operating efficiently at all other frequencies. Even in cases with a single dominant frequency, such as human walking gait, minor variations will still lead to suboptimal performance.

The near ubiquitous presence of physical vibration in a host of situations has lead many researchers to focus specifically on the problem of harvesting from oscillating mechanical motion. As virtually any device which undergoes circular motion at a fixed frequency will vibrate with an approximately sinusoidal displacement there is huge applicability for this type of system. The inclusion of systems experiencing free vibration from impulsive motion expands this. Even certain cases with constant inputs, such as vibration caused by aerodynamic flutter, are subject to harvesting [6]. For physical systems the primary approach to vibration-based harvesting is to devise a transducer that generates an electric potential by oscillating with the ambient source. The three most common transducers for this task are piezoelectric, electromagnetic, and capacitive, each of which shows a linear relationship between physical displacement and harvested power. This is the base excitation problem for single degree of freedom systems, depicted in Figure 1-1. As maximizing power is now dependent upon maximizing displacement (or velocity in the case of electromagnetic harvesters) systems are designed to have natural frequencies identical to the base motion. Physical damping is also minimized in order to maximize amplitude and improve efficiency.

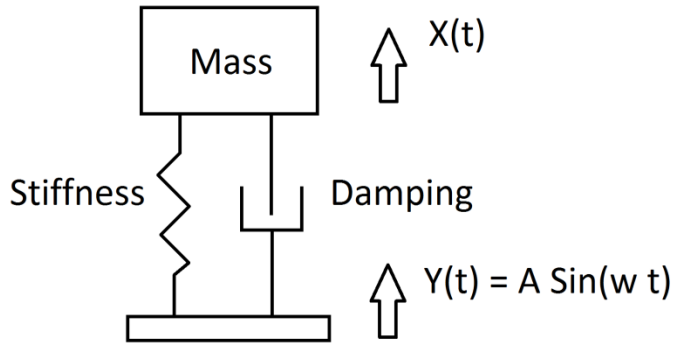

FIGURE 1-1: SINGLE DEGREE OF FREEDOM BASE EXCITATION WITH SINUSOIDAL INPUT

Although this approach is relatively straightforward to implement it presents a few problems that thus far have proven challenging to overcome, namely the narrow and highly sensitive effective frequency band.

Mathuna et al. [7] present power results for several different vibration harvesters reported in the literature. As vibration sources vary based on both amplitude and frequency for a fair comparison values have been normalized to a source acceleration of 1 m/s^2. Their data trends indicate that power levels are directly proportional to the volume of the device. A simple inspection of the governing equations describing power extraction for linear systems would indicate that higher frequency sources are more promising, however, this does not consider that in practice higher frequency sources oscillate with much lower amplitudes [7]. Taking this into account Mathuna et al. [7] show a relationship between power density and frequency that is roughly inversely proportional (on a log-log plot).

Mathuna et al. [7] lay out the problem of very narrow operational frequency bands for efficient vibration harvesting. "*In practice, a generator which has a more broadband response would be of greater practical use. However, there are, to-date, very few reports of such devices in the literature.*", "*The key challenges to be addressed are widening of the bandwidth of the device and a greater understanding of the parasitic damping issues so that the overall power densities can be improved.*"

Once the energy has been converted from mechanical to electrical new challenges arise. For vibratory and other alternating inputs the current is typically AC and so must be rectified and smoothed/regulated before it can be utilized by typical devices. The standard circuit model to perform this task is shown in Figure 1-2. It consists of an oscillatory source, full wave rectifier, and smoothing capacitor. Though often paired with piezoelectric vibration harvesters this circuit is equally applicable for use with any oscillating input, including those that are stochastic.

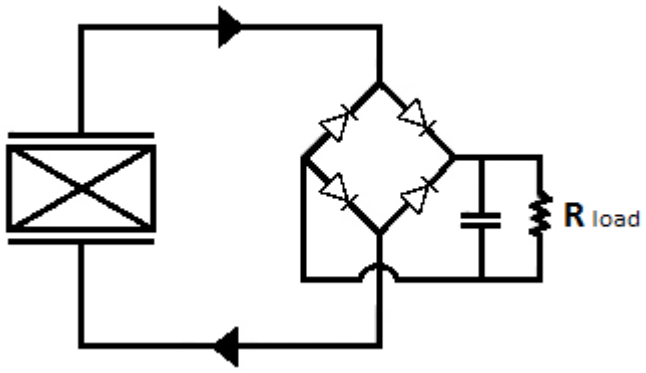

FIGURE 1-2: STANDARD MODEL OF VIBRATION ENERGY HARVESTING

With this model many researchers have made efforts to optimize and improve its performance. Shu and Lien [8] derive the optimal characteristics for a vibration based cantilever beam piezoelectric harvester. They are able to derive analytic expressions for the peak power harvested and the optimal load attached to the generator to accomplish this. The net result is that optimal power is extracted when the electrical load impedance is the complex conjugate of the input impedance [8]. While it is a thorough analysis of piezoelectric harvesters their focus is on how to optimize the operating conditions for a given harvester, rather than vice versa. In practical applications the source vibration is not a tunable parameter and neither is the load requiring power. In the case of WSNs, where much of the work done on energy harvesting sees real world applications, the sensor's power requirements are often already minimized and not easily lowered further. While an additional load may be placed in series to achieve the optimal total load (if it is higher than the present load) this serves only to increase the power extracted from the source, not the power supplied to the sensor; a superfluous accomplishment. Still, other researchers have built on this approach of modifying the electrical system characteristics to improve performance.

Lefeuvre et al. [9] evaluate the performance of several different harvesting electronic interfaces. These 'active interfaces', which respond to the generator by switching between operational states within one cycle, are evaluated next to the standard 'passive interface' model, which consists of only a rectification bridge and smoothing capacitor (Figure 1-2). As in their previous work [10], [11], where they first introduce the idea of synchronized switch harvesting with inductors (SSHI), They show that exploiting nonlinear processes can offer huge gains in terms of harvested power. They demonstrate that under certain conditions the total energy withdrawn from the environment can be increased by orders of magnitude by incorporating the modified Series-SSHI and Parallel-SSHI designs. Under identical input vibrations and electromechanical coupling factor active systems were shown to provide a maximum increase in power of 17 times the standard model [9]. Lefeuvre et al. [9] also demonstrate the substantial change in harvested power between constant force excitation and constant displacement excitation; the latter capable of producing roughly 2 orders of magnitude more power. As is common in the literature the excitation was produced by a controllable source to ensure a precise frequency, the resonance frequency of the device, is provided. This single frequency source that is tunable to the device in question is not the norm in practical applications where the situation is reversed and the device must be tuned. Again, it is clear that the recurring challenge with vibration harvesters is their narrow frequency band.

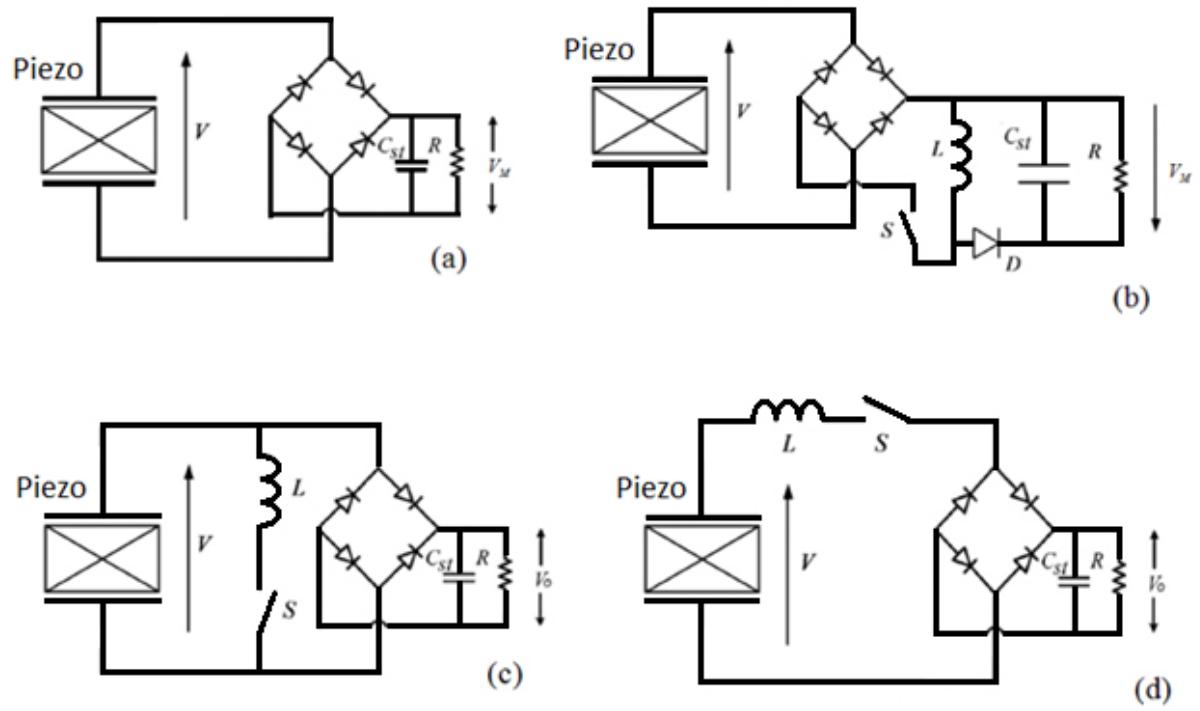

FIGURE 1-3: STANDARD HARVESTING CIRCUIT AND THREE NONLINEAR MODIFICATIONS. A) STANDARD MODEL. B) SWITCH PRECHARGED INDUCTOR. C) PARALLEL SSHI. D) SERIES SSHI. [9]

To directly address the problem of the high frequency sensitivity exhibited by vibration harvesters some proposed designs have focused solely on widening the effective bandwidth. Sharuz [12] actually considered the problem of an unknown or variable source vibration by designing a simple band-pass filter with a large frequency band. A generator like the one proposed by Sharuz [12] would consist of multiple beams, each tuned to a slightly different frequency to ensure operation over a wide range of source excitations. While effective, this approach is not ideal as a substantial number of beams are necessary - 21 beams are required to create a filter with a band of only 100 Hz [12]. Also, when excited by a single dominant frequency this approach ensures that the majority of beams within the generator will not be operating close to their optimal case. Even with low cost piezoelectric materials being commercially available, a method of greater utilization is desired.

Because cantilever beam scavengers are highly sensitive to the source vibration frequency several researchers have explored methods to widen the bandwidth of their devices. Challa et al. [13] were able to improve the bandwidth of a typical piezoelectric cantilever beam by 40% by utilizing permanent magnets mounted on and above/below the beam. By adjusting the distance between the magnets the magnetic force acting on the beam could be increased or decreased, effectively acting as an adjustable spring force which changed the resonant frequency of the system. This is an active tuning approach and requires manual adjustment. Further refinements could include a feedback mechanism to automatically adjust the magnet positioning, or the switch to electromagnets so their strength can be electronically controlled. These refinements would require utilizing some of the harvested power for an actuator or

for the electromagnets, reducing the overall system efficiency. A fully passive, unpowered tuning device is still desired.

Other solutions to the bandwidth problem propose self-tuning systems be designed. Researchers such as Ward and Behrens [14] have demonstrated wider effective bandwidth performance by deploying a reinforcement learning algorithm to control the resonant frequency of their harvester to an unknown, or possibly changing excitation frequency. The need for an external controller to monitor and adjust some parameter of the harvester adds an overhead power cost to these systems. Which has lead to researchers asking the question of whether a fully passive controller can be designed. This question has been answered as Scruggs [15] shows that for white noise excitation the optimal energy harvesting system cannot be achieved without an active controller.

As power input can vary greatly, power consumption also differs between systems. Not all systems can be classified as on-demand, in the sense that they only require power while human interaction is occurring. Some devices must continue operation during the periods without power input, necessitating that energy storage capabilities be present. The standard model does include a capacitor which offers minimal levels of storage. Increasing this capacitor size can offer greater storage, but at the cost of lower operating voltage for a given energy input and no longer having an optimal electronic load for maximum power extraction [16]. A simple move that would maintain a near constant operational voltage and allow for much greater energy storage is to include a chemical battery. The elimination of the reliance of battery usage is one of the primary arguments for energy harvesting technology, which makes their re-inclusion seem counterproductive. The argument must then be made that the two technologies work better in tandem than separately, at least in certain scenarios.

Thomas, Quidwai and Kellogg [17] evaluate potential harvesting methods to supplement power requirements for battery operated unmanned, autonomous vehicles. they were able to identify a number of potential sources and quantify the trade-offs between adding more batter mass/volume vs. adding harvesting mass/volume. Depending on the performance metric of interest - in their case flight time of a UAV - the potential benefits of adding more battery storage vs. more harvesting can be evaluated and compared. The trade-off between choices will likely depend heavily on the specific application and their analysis stopped short of a full optimization study.

1.5.RESEARCH APPROACH & CONTRIBUTION

In this regard an electronic door strike, or E-strike, can be classified as a WSN, as they are low power, intermittent, near an energy source, and autonomous. A rotational electromagnetic generator will be incorporated into the E-strike to harvest energy from non-periodic, fixed displacement mechanical motion. A full characterization of the energy flow through the system will be presented that could be applied to comparable impulsive motion harvesters.

While many different harvesting approaches exist in the literature and work has been done to optimize their performance the majority of mechanical motion harvesters are still frequency based and so rely upon constant input from a source within a narrow range of frequencies. Designs such as Lei Zuo's DC railroad energy harvester [18], who also designed what he refers to as a mechanical motion rectifier (MMR) are among the few frequency independent mechanical harvesters that have been proposed.

Furthermore, the question of energy storage has received little attention as it is often unnecessary in case where constant power is available, or is consumed immediately as in the wireless switch described previously [19]. In the majority of cases a simpler capacitor, which doubles as a smoothing capacitor, provides minimal storage capabilities, but is often sized to maximise energy extraction, rather than meet storage requirements [16]. The question of when to include a battery within a harvesting system, or whether a battery alone is the optimal choice will be answered for the case of electronic door strikes in Section 3.3. Similar analyses may be performed for other WSNs or smart devices as a primary design step.

In the case of electronic door strikes activation may require more power than can be applied at a given instant, necessitating the need to harvest and store energy over time. In the case of door strikes which harvest energy from door motion, the activation (unlock) will always preceded the input energy (door motion), again necessitating stored energy be ever present. The system may also sit idle for several hours or even several days. Over these time spans the assumption that electrical energy is stored indefinitely within a capacitor with no passive leakage through the bridge rectifier may not hold. A larger storage capacity would be needed to make up for such losses. The effect of this passive loss can be quantified and taken into account and its effect on system lifespan will be determined.

The inclusion of a chemical cell battery to address these issues adds complexity as the standard model of energy harvesting no longer suffices. Chemical batteries now have an associated energy conversion efficiency both when discharging and recharging [4]. Voltage and/or current regulation between harvester and battery are also necessary to prevent damage resulting from over-charging [20]. All cells have a non zero passive leakage current which slowly drains their energy, the value of which is dependent upon the cell chemistry employed [21]. Secondary cells also possess a maximum number of charge/discharge cycles before battery fatigue renders them unsuitable [22]. This cycle life is a function of both cell chemistry, as well as a host of other factors including depth of discharge, charge duration, charge frequency, current, voltage and temperature [22]. Identifying the parameters that have the largest effect on total system lifespan is a key step in characterizing performance.

There then likely exists an optima - or optimas - that maximises system longevity when these factors are accounted for. For example, is it more efficient to attempt to minimize the depth of discharge by passing small packets of charge frequently, or to reduce the charging frequency and number of cycles by first accumulating a larger charge bundle and then passing it into the cells? A hybrid energy harvester and secondary cell system model will be developed to qualify these relationships. Experiments are performed to validate this model. From this work appropriate charging parameters and cell types can be chosen to best suit different harvesting scenarios.

2. BACKGROUND & THEORY OF ENERGY HARVESTING

2.1. ENERGY SOURCES

Ambient energy exists throughout our environments in different forms. When implementing a harvesting device it is necessary to first identify all the potential energy sources. These different sources can be broadly grouped as thermal gradient, air current, photovoltaic, vibration, and electromagnetic fields. Paradiso and Starner [23] quantify typical available energy densities for different harvesting systems. Values are given per cm^2 or cm^3 in Table 2-1 for comparison:

TABLE 2-1 :POWER DENSITIES FROM DIFFERENT AVAILABLE SOURCES. VALUES TAKEN FROM [23]

Source	**Performance**
Ambient radio frequency	< 1 $\mu W/cm^2$
Ambient light (outdoors in direct sun)	100mW/ cm^2
Ambient light (indoors)	100 $\mu W/cm^2$
Vibration (human motion)	4 $\mu W/cm^3$
Vibration (mechanical equipment)	800 $\mu W/cm^3$
Ambient airflow	1 m $\mu W/cm^2$
Push buttons	50 μ J/N
Hand generators	30 W/kg
Heel strike while walking	<7 W

Not surprisingly, these estimates are far from certain and other researchers have also quantified the available power from different sources; often arriving at different values. Mathuna et al. [7] provides the following estimates in Table 2-2.

TABLE 2-2 : POWER DENSITIES FROM DIFFERENT AVAILABLE SOURCES. VALUES TAKEN FROM [7]

Source	Performance
Vibration	100 $\mu W/cm^3$
Ambient light (outside)	7500 $\mu W/cm^2$
Ambient light (inside)	100 $\mu W/cm^2$
Thermal gradient of 5°C	60 $\mu W/cm^2$

Matiko et al. [24] provide yet another estimate of harvestable energy:

TABLE 2-3 : POWER DENSITIES FROM DIFFERENT AVAILABLE SOURCES. VALUES TAKEN FROM [24]

Source	Performance
Ambient light (all sources)	9 - 399 $\mu W/cm^2$
Vibration (all sources)	0.05 - 459.8 $\mu W/cm^3$
Airflow	0.017 - 6.0 mW/cm^3
Thermal gradient	0.7 - 7.1 $\mu W/cm^3$
Electromagnetic/ Radio frequency	0.00169 - 57.37 nW/cm^3

The range of estimates can span orders of magnitude depending on the specific environment being considered. In the case of harvesting from human action the primary limit on peak power is governed by the level of burden one is willing to place on the end user. People are capable of generating substantial power, but may be adverse to the idea if it is unpleasant. A summary of power density estimates made by different researchers is presented in Table 2-4.

TABLE 2-4 : COMPARISON OF POWER DENSITY ESTIMATES. VALUES ARE NORMALIZED TO PER CM^3, OR CM^2 WHERE APPLICABLE

Source	Estimate					Minimum	Maximum
	Paradiso [23]	Mathuna [7]	Matiko [24]	Roundy [16]			
Ambient light (outside)	100 mW	7.5 mW	9 - 399 µW	15 mW		9 µW	100 mW
Ambient light (inside)	100 µW	100 µW	9 - 399 µW	10 µW		9 µW	100 µW
Vibration	800 µW	100 µW	0.05 459.8 µW	300 µW		0.05 µW	800 µW
Thermal	/	60 µW	0.7 - 7.1 mW	40 µW		0.7 mW	7.1 mW
EM/ Radio Frequency	< 1 µW	/	0.00169 - 57.37 nW	/		0.00169 nW	1 µW
Air flow	1 mW	/	0.017 - 6 mW	380 µW		0.017 mW	6 mW
Human action	4 µW, 7 W	/	/	330 µW		4 µW	7 W

These values can be visualized in graph form for clarity.

FIGURE 2-1 : RANGE OF POWER DENSITIES PROVIDED IN THE LITERATURE FOR DIFFERENT ENERGY SOURCES

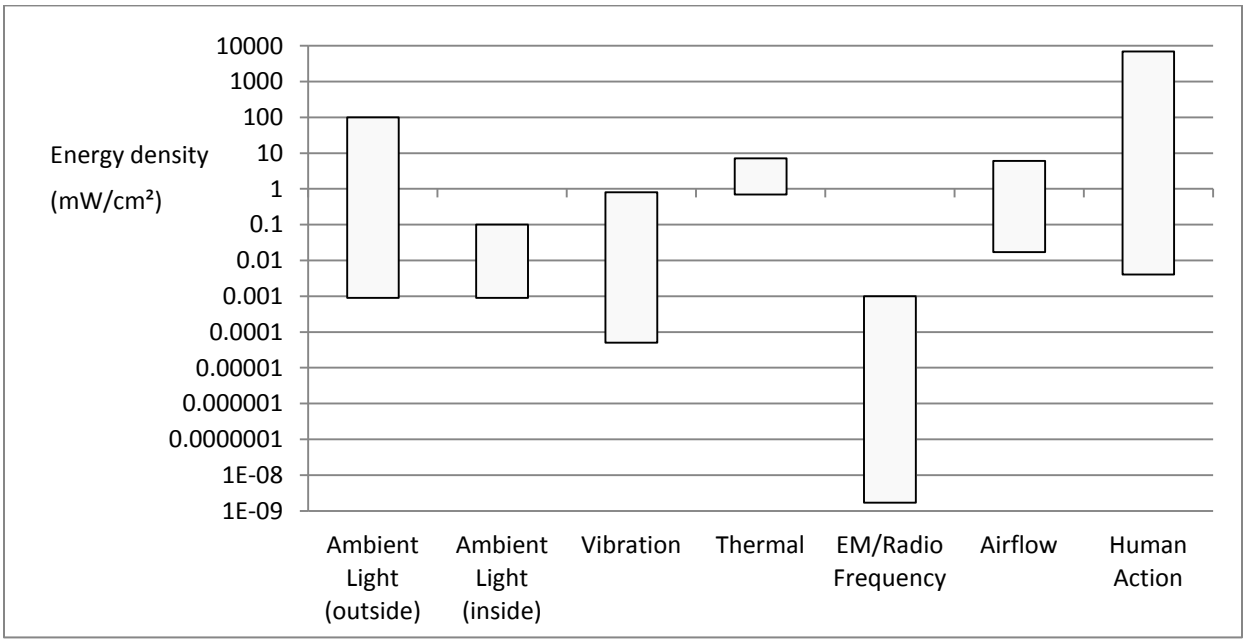

It is worth noting that while much work is being done the improvement of photovoltaic technology the light intensity from the Sun at the surface of the earth is 112 mW/cm^2 [25], and is presented as a theoretical upper limit on the available solar energy.

There exists a large degree of variability in power density from different sources due to the large number of different environments in which energy harvesters may be deployed. Ambient vibration may refer to highly active machinery in an industrial setting, or the considerably more gentle swaying of office buildings. Selection of an appropriate energy source when designing a harvester is confounded by the fact that the operating environment is often unknown a priori. For electronic door locks photovoltaic power densities can vary by 2 or 3 orders of magnitude based solely on if it is an interior or exterior facing door. While photovoltaic and vibration harvesters are often chosen due to the ubiquitous presence of either a light or vibration source in a great many environments, the energy density of those sources are uncertain. While either or both of these sources is likely to be present in most given environments their magnitudes are still highly variable. For systems where power failure is not acceptable a source that is both power dense and reliably present is necessary. The only effectively guaranteed and consistent energy source, in the case of door usage, is human interaction. Human action also offers the highest potential energy density of all sources identified. These two factors make human action the most suitable source for powering an electronic strike. The next matter is then determining how best to extract this energy.

2.2.HARVESTING METHODS

Different sources will necessitate different harvesting methods. One of the most commonly seen harvesting methods is photovoltaic. A popular choice, it is often billed as a highly environmentally friendly alternative to fossil fuels and nuclear power. From an end user's perspective photovoltaic cells are simple and straightforward to integrate as a power source as one need only connect the positive and negative terminals of each cells to the respective circuitry component. As was seen in Section 2.1 available energy densities vary widely for ambient light sources, especially between indoor lighting and direct sunlight. Not only does the intensity of light vary, but the nature of it does as well. The frequency spectrum of natural sunlight is much broader than typical fluorescent lighting. Therefore the power density of indoor lighting is concentrated into specific frequencies. Specific cells must then be chosen that are designed to operate optimally under different spectra. Once again the choice of optimal harvesting method is case specific.

Physical motion likewise exists with different properties. For the often studied case of single frequency vibration both the frequency and amplitude will vary across scenarios. The method chosen to acquire this energy also presents multiple options. When harvesting from physical motion piezoelectric transducers are often used as they provide high voltage values that often do not need to be stepped up to usable levels [16]. They are also mechanically simple, typically consisting of a cantilever beam, proof mass, and bridge rectifier circuit. Extensive analysis has been done on piezoelectric harvesters, their design, modes of operation and optimization. A full review of this technology is beyond the scope of this work, but suffice it to say the majority of the research on piezoelectric harvesting is done on periodic vibration sources. Impulse excitation is much more rarely considered, with a few notable exceptions, such as the footfall apparatus of [26].

Some harvesting systems are entirely physical in nature, such as the self winding wrist watches that are commercially available. An oscillating mass on a unidirectional sprocket can progressively wind a spring that slowly dissipates its stored energy as the watch ticks. This motion caused by an oscillating mass is force based, and so it's amplitude decreases as the stored energy in the spring increases and its reactive force rises. The energy input per human motion is then a decreasing function of the amount of currently stored energy. Slightly modified versions of this replace the winding of a spring with the motion of a magnet next to a wound coil to generate an electric potential. While during walking the swaying of a wrist may be periodic, most human motion is far more complex and not easily modelled.

Capacitive motion harvesters also exist and operate on the same principle as piezoelectric and electromagnetic vibration systems. Capacitive vibration harvesters have even been manufactured at the MEMS scale, allowing for harvesting of the tiniest of motions. Their largest drawback is the need to apply a pre-existing voltage across the capacitor for operation. This approach may integrate well into MEMS power systems, but does not scale to larger applications where higher voltages than can normally be attained with capacitive type harvesters are necessary.

Piezoelectric materials can also be fabricated within MEMS and can be used to similar effect as capacitive harvesters. While piezoelectrics can be deployed in both micro and small scale (millimeter and centimeter) to generate significant voltages from motion increases in size can reduce their applicability. The typically higher power densities exist at lower excitation frequencies [7] which for cantilever beam harvesters necessitates either a very long beam or very large proof mass to match the source and harvester resonant frequency.

For base excitation the relative motion between the base and oscillating mass is linearly related to the base amplitude. While increasing the displacement of a cantilever beam harvester, whether it be piezoelectric or capacitive, will lead to increases in voltage and hence extracted power, it can also decrease the product lifespan by increasing material strain and stress. Two sources with the same frequency will provide different power levels and may or may not damage the harvester, depending on their amplitude. Clearly a harvester that quickly undergoes material failure is counterproductive to the primary goal of achieving and infinite power supply lifespan. A line must then be walked between operating at a high enough displacement that meaningful power levels are obtained, but low enough that material strain and stress are kept to within acceptable limits. This problem is easily solved when the source amplitude is known precisely, but this is not always the case.

Piezoelectric generators have been shown to outperform other vibration harvesting methods such as oscillating electromagnetic and capacitive types [16], but when applied to impulse sources can lead to unreasonable physical design requirements. Experiments conducted on a piezoelectric cantilever beam (Volture V25W Piezoelectric Energy Harvester [27]) excited by an impulse input of known displacement offer an illustrative example:

A piezoelectric beam with a stiffness of approximately 600N/m was deformed at its tip by 2mm, its peak deflection prior to material failure. The beam was then released and allowed to oscillate freely at its natural frequency. Peak recorded voltage levels were 14V, with electrical energy harvested values of 0.57mJ, corresponding to a conversion efficiency of 52.2%. This system has a natural frequency of 355 rad/s at its peak efficiency. Scaling this system to operate with an input energy of 564mJ requires maintaining the same natural frequency. For the same piezo transducer to deform by 2mm and accept an input energy of 564mJ its stiffness would need to be increased to 282 N/mm. Maintaining a natural frequency of 355 rad/s requires a tip mass of 2.24 kg, which is impractically large to contain within a door strike. A more volumetrically dense conversion technique is necessary.

2.3. ROTATIONAL AND IMPULSIVE INPUT METHODS

Some researchers have focused on extracting power from rotational motion and so design and build electromagnetic micro generators, rather than cantilever beams. These designs typically operate at very high rotational speeds, ranging from 4000 RPM to 380 000 RPM [28]. The small form factors and high required speeds may make them suitable for high frequency vibration harvesting if a suitable method of conversion between vibrational motion and angular motion is devised. High frequency low amplitude vibration is far more common than the more sought after low frequency vibration, but is also typically less energy dense [29]. If a vibration-to-rotation device were paired with a micro generator such as one of these many previously untapped vibration sources would become viable.

Rotational motion harvesting has been explored to a small extent. Dubbed a 'gravitational torque generator', efficient rotational harvesting over a bandwidth of 6000 RPM has been demonstrated [30]. Converting vibration to rotation with the use of an eccentric mass rotating about a generator shaft has been proposed as well [31], but thus far has not seen further development. The E-rotor concept presented in [31] demonstrated a self-tuning property to different vibrating frequencies which is highly desirable and not typically present in oscillating harvesters. This E-rotor concept is in principle capable of generating a maximum power equal to that of oscillating harvesters, with the added benefit that power scales with frequency cubed so long as the rotor and base frequencies remain in sync [31]. This approach does however require a control circuit to 'lock-in' full rotation at a given frequency otherwise synchronization with the base motion may be lost. the average power extracted will then be zero without electronic rectification.

Mechanical action is certainly not limited to sinusoidal, or even oscillating motion. Actions such as pressing a button or typing on a keyboard are inherently impulsive, with no clear dominant frequency or smooth motion. Like typing on a keyboard, many of these impulsive motions are the result of human actions. Since many devices such as switches, keyboards, mice, and door locks only require power during human interaction people are a natural source of energy to exploit. A clear example of one such device that is reaching wider use is the wireless switch developed by Cherry [19], which transmits a radio frequency signal entirely powered by button motion.

Other researchers have devised systems that gather energy from prosthetic feet [32]. The conversion method used is a rotational electromagnetic generator. The generator is activated by a ball screw that converts linear oscillation to rotational oscillation. Their prototype could generate a peak voltage of 7.7V, and an average power of 797mW (averaged over one step cycle). This corresponds to a volumetric power density of 6.28mW/cm^3. This voltage and current needed both rectification and regulation to 3.3V to power their system which thus incorporated additional losses in power. These power losses were not quantified, but removal of the need to rectify a source is likely to improve overall performance.

With so much prior work existing regarding vibration harvesting there have been attempts to adapt these approaches to impulse sources. Starner and Paradiso [33] consider using piezoelectric materials to harvest the impulse from foot fall impact. They were able to harvest peak powers of 60 mW, with an average of only 8.4 mW over a step period. Their mechanical to electrical conversion efficiency was only about 1%, which is substantially lower than values attainable from periodic vibrations using similar

piezoelectric materials, but may be kept intentionally low to ensure the device does not create an undesirable load on the user. A number of researchers, such as Gilbert and Balouchi [26] have proposed using impulse inputs to oscillate a cantilever beam at its natural frequency. This approach allows some other techniques developed for vibrational inputs to be applied. There would no longer be a base frequency that dictates design and frequency matching need only consider the mechanical to electrical conversion. Systems such as this will always oscillate at their natural frequency. Though impulsive inputs are inherently less power dense than comparable source vibration they can provide higher total energy. Gilbert & Balouchi [26] use a vibrating cantilever coil between permanent magnets to harvest AC power. They were able to get 60mJ/step, or approximately 60mW. They claim their system can scale to 2.75 W/m^3 ($0.00275mW/cm^3$).

As the E-strike is not subject to periodic vibration, but instead is provided with infrequent impulsive motion of a known displacement a typical resonance-based harvester is not particularly well suited. This rules out drawing from the literature on frequency matching techniques to improve performance. It is important to note that the input is displacement based, rather than force based, which can allow for greater energy extraction. A simple estimate for the maximum available energy from a known linear or rotational displacement, respectively, is:

$$Energy = Force \cdot Displacement$$

$$Energy = Torque \cdot Angle$$

Where the force and torque terms can be chosen by the designer. This implies there is no physical limit to the upper bound of energy per input, there are only case dependent practical considerations to be made. Fixed displacement inputs relax many of the requirements common to physical motion harvesters, such as the need for resonance tuning and the presence of a proof mass. this can allow for simpler electronic components and much smaller form factors. The known displacement also ensures there is a known maximum strain on any deflected components. The electrical load applied to a harvester typically has the effect of damping physical motions by applying a resistive force to the mechanical displacement. For a fixed displacement at a presumably constant velocity this leads to an increase in the resistive force the human operator must overcome, which must be accounted for in the design process.

When analyzing the energy throughput of a system it is important to look not only at the average power provided and consumed over long periods, but the instantaneous power of the system as well. Large spikes in the incoming power may not be captured and stored efficiently. Similarly the instantaneous power needs of an electronic device will pose a more stringent requirement on a harvesting system than the time averaged power needs. Impulsive systems with infrequent activations face both of these challenges. The amount of power available from human interaction is dependent upon the frequency of interaction, as is the power consumption. For these reasons energy input per interaction and energy output per activation will be the metrics under investigation. Hence forth these values will be referred to as 'input energy', and 'activation energy', respectively.

3. HYBRID SYSTEMS

3.1.THE NEED FOR BATTERIES

With much of the research work focusing on energy extraction the question of energy storage is often not addressed. For continuous sources that are paired with continuous power consumption, as is the case with some WSNs, a simple capacitor is often sufficient to handle minor temporary fluctuations in electrical power supplied. Even stochastic inputs may have low storage requirements when sources are ever-present. Impulsive motion harvesters, specifically those that operate from infrequent impulsive motion, must either use the energy immediately, as the radio frequency switch harvester does [19], or store a substantial quantity for a later time. E-strike operation cannot be predicted accurately in many situations, owing to the huge number of different situations that one may be positioned in. A door may be opened hundreds of times an hour, then sit idle for several days. If a passive harvester such as a photovoltaic cell is used the energy collected over these several days must all be stored in order to accommodate the busier periods.

Even if it is assumed that the incoming energy is equal to the outgoing required energy when both are averaged over long periods of time the fact that these quantities are relatively large impulsive bursts will still necessitate that a large energy store be present. It is clear that for large energy inputs or outputs a capacity of at least the maximum of either the energy in or energy out is necessary. The situation is confounded when the inputs and outputs are more sporadic. If the input and output occur in one-to-one parings the storage capacity is simply the maximum of the system energy change, but when these events do not coincide in one-to-one pairs the required capacity can increase dramatically, as exemplified in Figure 3-1. In each case the average energy coming into and being consumed is identical over the time span shown.

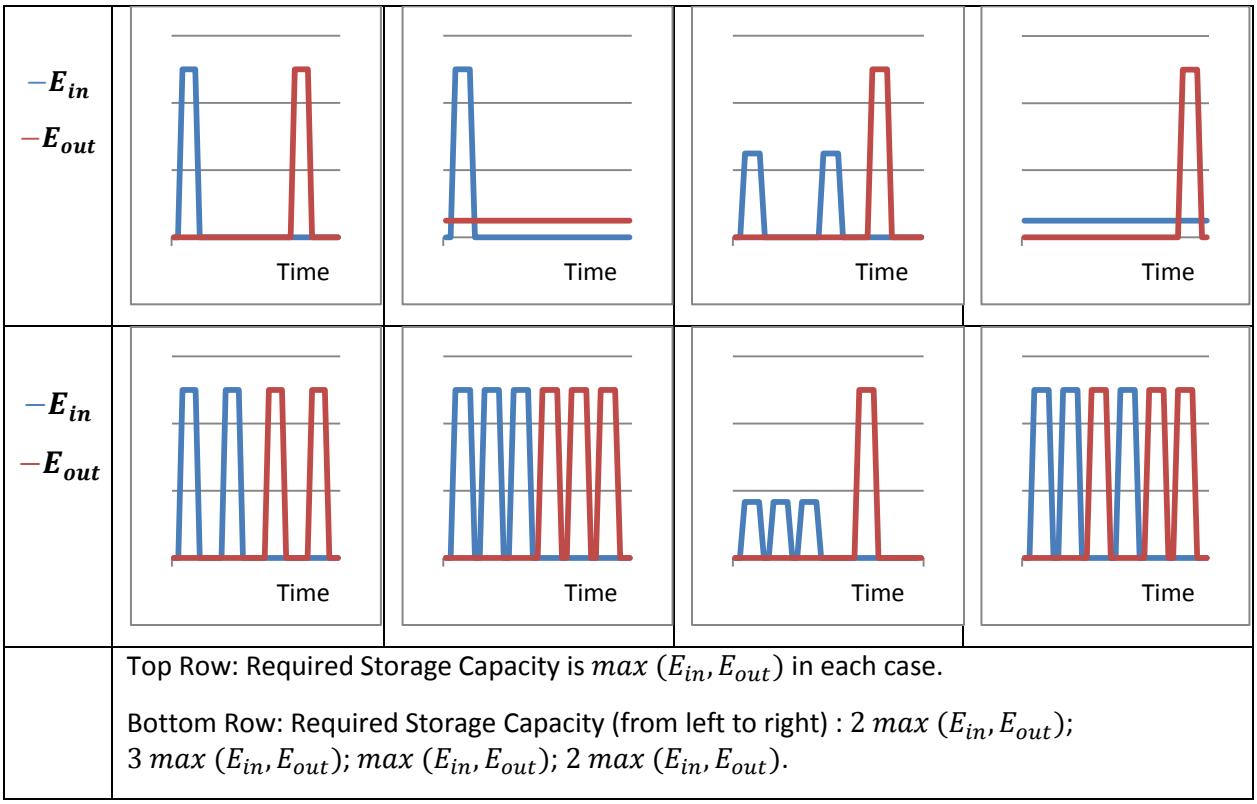

Top Row: Required Storage Capacity is $max\ (E_{in}, E_{out})$ in each case.

Bottom Row: Required Storage Capacity (from left to right) : $2\ max\ (E_{in}, E_{out})$; $3\ max\ (E_{in}, E_{out})$; $max\ (E_{in}, E_{out})$; $2\ max\ (E_{in}, E_{out})$.

FIGURE 3-1: POSSIBLE ENERGY FLOW CASES IN A SYSTEM WITH EITHER CONSTANT OR IMPULSIVE INPUT AND OUTPUT

For impulsive energy input and consumption the battery capacity necessary to ensure operation will be equal to the largest number of unaccompanied activations that occur in a row. Assuming one of two possible discrete events may occur at a given instant we wish to know the probability over a given period of time that a long streak of activations will occur.

In the most general case where input and output events are uncorrelated and random correctly sizing a battery that is able to both store all the incoming energy and meet all the energy demands can be expressed as a probability function. This is done by calculating the likelihood that a streak of at least K activations occurs in a row in a series of N events, without an input occurring. The probability of a streak of activations of a certain size occurring increases as the operational life increases and tends toward 1 as the lifespan approaches infinity. The Absolute maximum storage capacity that could be used is simply equal to the activation energy multiplied by the total number of events, which assumes no input ever occurs. A more reasonable assumption would be that activations and inputs occur in approximately equal amounts.

The probability, S, of a streak of activations of a certain size K is then expressed by the equation [34]:

$$S(N,K) = p^K \sum_{T=0}^{T=\infty} \binom{N-(T+1)K}{T} (-qp^K)^T - \sum_{T=1}^{T=\infty} \binom{N-TK}{T} (-qP^K)^T$$

Where p is the probability of an activation occurring, K is the size of the streak, and N is the total number of events that may occur. q is the probability of an input occurring ($q = 1 - p$). The 'choose function' within the summation, denoted $\binom{A}{B}$, is assigned the value of zero when $A < B$ as there cannot have a streak of K larger than N.

A battery can then be sized by choosing reasonable values for the probability of p with respect to q. The value N may be chosen by estimating a non-infinite product lifespan and the associated input and activation frequencies. Sample probability values are shown in Table 3-1 for the case where inputs and activations occur with equal likelihood.

TABLE 3-1: PROBABILITY OF HAVING A STREAK OF K ACTIVATIONS AS LIFESPAN INCREASES. $p = 0.5$

		Streak length, K									
		1	**2**	**3**	**4**	**5**	**6**	**7**	**8**	**9**	**10**
Number of events, N	**1**	0.5									
	2	0.75	0.25								
	3	0.875	0.375	0.125							
	4	0.9375	0.5	0.1875	0.0625						
	5	0.9688	0.5938	0.25	0.0398	0.0313					
	6	0.9844	0.6719	0.3125	0.125	0.0469	0.0156				
	7	0.9922	0.7344	0.3672	0.1563	0.0625	0.0234	0.0078			
	8	0.9961	0.7852	0.4492	0.1875	0.0781	0.0313	0.0117	0.0039		
	9	0.9980	0.8262	0.4648	0.2168	0.0938	0.0391	0.0156	0.0059	0.002	
	10	0.9990	0.8594	0.5078	0.2451	0.1094	0.0469	0.0195	0.0078	0.0029	0.001
	50	1.000	1.000	0.9827	0.8274	0.5519	0.3146	0.1653	0.0836	0.0415	0.0204
	100	1.000	1.000	0.9997	0.9727	0.8101	0.5461	0.3175	0.1702	0.0876	0.0441
	500	1.000	1.000	1.000	1.000	0.9998	0.9832	0.8636	0.6251	0.3849	0.2145
	1000	1.000	1.000	1.000	1.000	1.000	0.9997	0.9818	0.8611	0.6242	0.3854

As can be seen, even with approximately equal input and output energy, or neutral power flow, there is still a need for significant energy storage capacity. Within only 1000 events - a value that could be seen by one door in a single day - there is a nearly 40% chance that enough stored energy must be available to power 10 activations. Strictly speaking, a super capacitor can hold this energy, but will not possess a flat voltage-energy curve. This leads to a large amount of energy being stored at voltage levels too low for practical use. In this regard a chemical battery is advantageous.

While there is a closed form expression to determine the required battery size in this most general of cases with stochastic input and activation patterns, the matter can be simplified when dealing specifically with E-strikes. For door motion it is reasonable to assume that the number of openings will

always be greater than or equal to the number of unlockings. In fact, an activation-per-input ratio of 1.0 is the worst case scenario and it is more often the case that this ratio will be much lower. If it is assumed that the input energy is greater than or equal to the activation energy of the E-strike and activation-per-input ratio never exceeds 1.0, then the average energy flow through the system will always be positive and an infinite system lifespan is ensured.

The last assumption, that sufficient energy is harvested from one input to power one activation must then be evaluated. If this assumption is not held then an infinite lifespan cannot be guaranteed, but may still be possible to achieve under certain operating conditions. For any system with a negative energy flow a larger battery capacity will always be necessary to maximize lifespan.

3.2. CELL CHEMISTRIES OVERVIEW

With the size of battery selected the specific cell chemistry also plays a role. Different chemistries operate at different voltage potentials, have different stored energy densities, as well as different rates of passive energy loss over time which is referred as a battery's self discharge rate. Nominal values for common chemistries are shown in Table 3-2.

TABLE 3-2: TYPICAL BATTERY TYPE PERFORMANCE PROPERTIES

Battery Type	Voltage [V]	Energy density [MJ / L]	Self-Discharge [% / month]	Cycle durability
Lead–acid	2	0.27	3	800
LiFePO4	3.2	0.79	4.5	7500
LiPo	3.7	2.23	5	1000
Lithium	3	2.1	1	1
Lithium-ion	3.7	2.23	8	1200
Low self-discharge NiMH	1.2	1.1	0.9	1800
Nickel–iron		0.108	20	5000
Nickel–metal hydride	1.2	1.08	30	1000

With a high capacity battery the question can be asked if a harvesting system is still necessary. Or, rather, what is the incremental improvement by including a harvester? If no harvesting system is present then the energy storage device need not be rechargeable and a standard primary chemical battery will suffice. Many different chemistry types are available, from lead-acid to lithium ion, and each

is better suited for different applications. All chemical batteries slowly lose their stored energy over time, with different chemistries possessing different storage characteristics [21]. The most important requirement would be a low self-discharge rate and maintaining a minimum voltage of at least 3V to operate the E-strike circuitry and motors. In this regard lithium chemistries are ideal as they only discharge at a rate of 1-3% per month [35], half the rate of lead acid chemistries and far below nickel based reactions [35]. Several commercially available lithium based batteries are shown in Table 3-3 with their corresponding energy density and approximate number of door strike cycles that can be executed.

TABLE 3-3: TYPICAL PRIMARY LITHIUM BATTERIES WITH FORM FACTORS SUITABLE FOR DOOR STRIKE APPLICATION

Capacity [mAh]	Size / Dimensions	Volume [mm^3]	Energy Density [mAh / mm^3]	Operations
240	20.0mm^2 x 3.2mm	1005.30	0.2387	6067
560	23.0mm^2 x 5.4mm	2243.57	0.2496	14156
620	24.5mm^2 x 5.0mm	2357.18	0.2630	15672
1000	24.5mm^2 x 7.7mm	3630.05	0.2755	25278
3300	29.0mm x 14.5mm x 52.0mm	21866	0.1509	83418

As can be seen from Table 3-3 primary batteries capable of 25000 cycles are readily available with form factors that fit well within a normal strike envelope. Note that this estimate of the number of cycles does not take into account self-discharge or any inefficiencies that will exist. The operational lifespan of a battery-only door strike, measured in months or years, will then depend on the frequency of use.

TABLE 3-4: TYPICAL NICKEL METAL HYDRIDE SECONDARY BATTERIES WITH FORM FACTORS SUITABLE FOR DOOR STRIKE APPLICATION

Capacity [mAh]	Size / Dimension	Volume [mm^3]	Energy Density [mAh / mm^3]	Operations
930	10.5mm^2 x 44.5mm	3853.26	0.2414	7836
1900	14.2mm^2 x 50.4mm	7981.73	0.2380	16009
2100	17.0mm^2 x 50.0mm	11349	0.1850	17695
3000	23.0mm^2 x 43.0mm	17865.45	0.1679	25278
3600	17.0mm^2 x 67.5mm	15321.15	0.2350	30334
4200	18.2mm^2 x 67.0mm	17430.4	0.2410	35389

Attaching a form of energy harvesting system has the potential to significantly increase the lifespan of any battery powered device, but requires that a rechargeable secondary battery be used. The energy densities of secondary batteries are different due to their different chemistries. Typical secondary batteries and their expected number of cycles - not considering recharging - are shown in Table 3-4.

Capacities comparable to primary cells are available in rechargeable batteries as well. The drawback typically associated with secondary batteries is their substantially higher self-discharge rate. This passive loss can be quite significant and may not be fully offset by a harvesting system, specifically for Nickel-Metal-Hydride (NiMH) rechargeable chemistries, which can lose up to 50% of their stored energy within six months . As an illustrative example, the expected lifespan, measured in months, for several different primary and secondary batteries is shown in Figure 3-2 in Section 3.4. Corresponding battery properties are presented in Table 3-7.

3.3.PRIMARY VS. SECONDARY CHEMISTRIES

It has been shown that for impulsive harvesting a battery is typically necessary , particularly when the energy quantities are relatively high. The converse statement that a harvesting system is necessary to pair with a battery has not yet been shown and is the subject of this section. By varying the operating parameters of the harvester, specifically the activation frequency and harvesting efficiency, and calculating the E-strike life span in months a direct comparison between primary battery and a secondary battery plus harvester can be made.

An estimate for the charge, Q_t, remaining in a battery after a certain time can be iteratively calculated by:

$$Q_t = Q_{t-1}(1 - L) - N(E_A - E_I\varepsilon) - c$$

Where L is the self-discharge, or leakage rate as a percentage of state of charge, N is the number of operations that occur between time t and $t - 1$, E_A and E_I are the activation and input energies, respectively, ε is the harvesting efficiency, and c is a continuous power draw that models a low power radio receiver.

Using the values of $E_A = 430$ mJ, The quantity needed to power the strike circuitry, and $E_I = 0.564J$, which is the maximum available energy derived in section 0. The L term is as listed for each battery, and $c = 139968mJ$ per month (54µW) which is an estimate provided by [7]. The activation frequency, measured in activations per month, was varied between 150 and 1200, as was the harvesting efficiency. At each combination of harvesting efficiency and activation frequency either a primary battery or secondary battery and harvester will provide the maximum life span. The lifespan of a series of secondary batteries with harvester, compared to a non-rechargeable primary lithium batteries is shown in Figure 3-2.

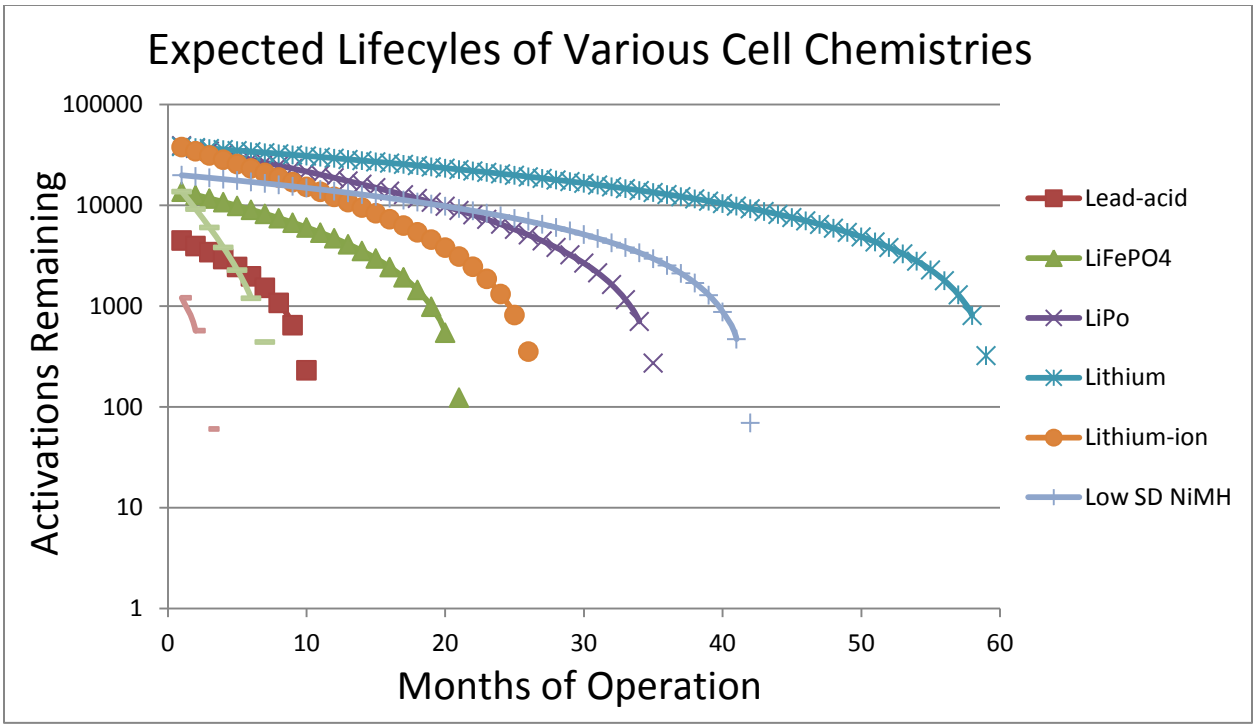

FIGURE 3-2: EXPECTED LIFECYCELS OF VARIOUS CELL CHEMISTRIES. 150 ACTIVATIONS PER MONTH, 40% HARVESTING EFFICIENCY.

Because different chemistries possess different energy densities cell capacities have been normalized to a volume of approximately one standard 'A' battery. Energy expenditures from the cell include the activation energy (430mJ per operation), continuous self-discharge, and an estimated standby power of 54µW while not active [7].

With 40% overall harvesting efficiency the highest performing battery is the non-rechargeable Lithium cell. While both the rechargeable Lithium-ion and Lithium-Polymer (LiPo) have nearly identical initial energy, their self-discharge rates are substantially higher. The best performing rechargeable battery is the low self-discharge (low SD) nickel metal hydride. While initially these findings suggest a single non-rechargeable battery is the optimal choice this analysis is very sensitive to a number of factors including the initial battery volume, standby power consumption and energy harvesting efficiency. Minor modifications to any of these factors changes the relative performance of each cell chemistry and hence the choice of optimal battery. In general either the primary lithium, low SD NiMH, or LiPo battery will be the top performer.

This calculation can be repeated across a range of different monthly activation frequencies and harvesting efficiencies to identify which scenarios will lead to a hybrid harvesting system outperforming a standalone battery. The results are tabulated in Table 3-5.

TABLE 3-5: OPTIMAL SYSTEM CHOICE BASED ON ACTIVATION FREQUENCY & HARVESTING EFFICIENCY

	Harvesting Efficiency							
Activations per month	**20%**	**30%**	**40%**	**50%**	**60%**	**70%**	**80%**	**90%**
150	Primary	Primary	Primary	Primary	Primary	Primary	Primary	Primary
200	Primary	Primary	Primary	Primary	Primary	Primary	Rechargeable	Rechargeable
250	Primary	Primary	Primary	Primary	Primary	Rechargeable	Rechargeable	Rechargeable
300	Primary	Primary	Primary	Primary	Primary	Rechargeable	Rechargeable	Rechargeable
350	Primary	Primary	Primary	Primary	Rechargeable	Rechargeable	Rechargeable	Rechargeable
400	Primary	Primary	Primary	Primary	Rechargeable	Rechargeable	Rechargeable	Rechargeable
450	Primary	Primary	Primary	Primary	Rechargeable	Rechargeable	Rechargeable	Rechargeable
500	Primary	Primary	Primary	Primary	Rechargeable	Rechargeable	Rechargeable	Rechargeable
550	Primary	Primary	Primary	Rechargeable	Rechargeable	Rechargeable	Rechargeable	Rechargeable
600	Primary	Primary	Primary	Rechargeable	Rechargeable	Rechargeable	Rechargeable	Rechargeable
1200	Primary	Primary	Rechargeable	Rechargeable	Rechargeable	Rechargeable	Rechargeable	Rechargeable

An interaction was found between activation frequency and harvesting efficiency. As harvesting efficiency increases rechargeable system performance begins to surpass primary batteries, but only at higher uses. For efficiency levels below 40% a primary battery always outperforms a rechargeable system. Not surprisingly, more frequent use decreases the lifespan of both primary and rechargeable systems. Self-discharge was also found to have less of an impact as activation frequency increased, due to the decreased lifespan. The relative impact of these other factors is investigated in greater detail in section 3.4.

Values in Table 3-5 assume that both batteries have equal volume, and the volume of the harvesting unit and added circuitry is neglected. This harvesting component volume may however not be negligible. Size constraints are an important consideration in many systems that may potentially benefit from energy harvesting. When utilizing energy sources such as ambient vibration or photovoltaic panels it is often possible to increase the amount of energy gained by an arbitrarily large amount simply by increasing the size or number of harvesting devices. While at times beneficial, this approach is often impractical as it does not lend itself to a fair comparison of energy sources. To allow for a valid comparison of energy sources it is useful to work in terms of power density - or energy density in the case of batteries. Battery energy densities, in milliamp-hours per mm^3, for various cell chemistries were presented in Table 2-2 and Table 2-3. These can be viewed alongside our chosen energy harvesting method, which can be quantified based on its power density in mW per mm^3. Since energy harvesters repeatedly harvest energy from an environmental source their energy density is technically infinite

when viewed over an unbounded time span. To compare to a battery of limited volume an operational lifespan must be chosen. For this analysis a minimum lifespan of 24 months was chosen.

A fair comparison of primary batteries and harvesting systems can be done by assuming that our electromagnetic harvesting system could be replaced by a primary battery of equivalent size. For this comparison a high grade compact rotational generator with a volume of approximately 13 000mm^3 is used (length of 34mm, diameter of 22mm). This volume can potentially be replaced by a primary cell. Table 3-6 shows the optimal case for when a single 'A' size battery with an effective volume of approximately 8000mm^3 is paired with a harvesting system of 13000mm^3, compared to a single primary battery with a total volume of 21000mm^3.

TABLE 3-6: OPTIMAL SYSTEM CHOICE BASED ON ACTIVATION FREQUENCY & HARVESTING EFFICIENCY FOR EQUIVALENT VOLUME SYSTEMS

	Harvesting Efficiency							
Activations per month	**20%**	**30%**	**40%**	**50%**	**60%**	**70%**	**80%**	**90%**
150	Primary	Primary	Primary	Primary	Primary	Primary	Primary	Primary
200	Primary	Primary	Primary	Primary	Primary	Primary	Primary	Primary
250	Primary	Primary	Primary	Primary	Primary	Primary	Primary	Primary
300	Primary	Primary	Primary	Primary	Primary	Primary	Primary	Primary
350	Primary	Primary	Primary	Primary	Primary	Primary	Primary	Primary
400	Primary	Primary	Primary	Primary	Primary	Primary	Primary	Primary
450	Primary	Primary	Primary	Primary	Primary	Primary	Primary	Rechargeable
500	Primary	Primary	Primary	Primary	Primary	Primary	Primary	Rechargeable
550	Primary	Primary	Primary	Primary	Primary	Primary	Primary	Rechargeable
600	Primary	Primary	Primary	Primary	Primary	Primary	Rechargeable	Rechargeable
900	Primary	Primary	Primary	Primary	Primary	Rechargeable	Rechargeable	Rechargeable
1900	Primary	Primary	Primary	Primary	Rechargeable	Rechargeable	Rechargeable	Rechargeable

For efficiency values below 60% a primary battery will outperform a harvesting system paired with a rechargeable battery. Only at very high efficiencies and at very high activation frequencies will a harvesting system make up for the much lower initial capacity of a rechargeable battery.

For a harvesting system of size 13000mm^3 to be on par with a primary lithium battery with typical energy density of 2100mJ/mm^3, when extracting energy from an impulse load of 572mJ, the harvesting system must be at a minimum 60% efficient. Conversely, if more reasonable efficiency values of 40% are assumed, then a harvester and corresponding hardware must be made to fit within 1500mm^3 and have an activation frequency of at least 1400 per month for equivalent performance to a primary battery.

Depending on the desired product lifespan an energy harvesting system may not be necessary. Prior to implementing a harvester it is useful to evaluate the performance of a single non-rechargeable, or primary, battery to see if one can be found that meets requirements. Even if a harvester is deemed necessary a design based on a primary battery serves as a useful baseline for comparison and offers a means to quantify performance benefits.

This analysis indicates that a primary battery will generally outperform a rechargeable system in infrequent use applications, and a hybrid system is optimal in high frequency use applications . A more in depth investigation was performed to identify exactly where this transition between primary and rechargeable system optimality occurs. In all cases either a primary lithium ion battery, or a low self-discharge nickel-metal-hydride (low SD NiMH) paired with a harvesting system were found to be optimal. The following analysis focuses on comparisons between these two systems.

3.4.LIFESPAN CALCULATIONS & COMPARISON

This analysis thus far assumes a one-to-one paring of input energy to lock/unlock activation, which is not representative of most E-strikes. In fact it is the worst case scenario as typically doors may be opened dozens, or even hundreds, of times without being activated. A model specific to the door strike can be developed. First, a number of key terms must be defined.

At any given instant an estimate of the number of remaining activations is given by:

$$N = \frac{E_{B(t)}}{E_A}$$

Which corresponds to a timespan estimate of:

$$T = N/\omega_A$$

Which does not directly account for passive leakage. The instantaneous battery energy, $E_{B(t)}$, is a function of its inital charge, E_{B0}, input energy, E_I, output energy, E_A, their respective input and activation frequencies, ω_I, and ω_A, and passive leakage, L.

$$E_{B(t)} = E_{B0} + \varepsilon \times E_I \times \omega_I \times t - E_A \times \omega_A \times t - L \times E_{B(t)} \times t$$

Rearranging:

$$E_{B(t)} = \frac{E_{B0} + \varepsilon E_I \omega_I t - E_A \omega_A t}{1 + Lt}$$

Where it is assumed that ω_I and $\omega_A$are approximately constant over long periods, or can be taken as averages over time.

It is also assumed that the passive leakage, L, is linearly related ot current battery charge. Other models may include modelling passive leakage as proportional to initial charge, rather than current charge, $E_{B(t)} \propto LE_{B0}t$. For our purposes choosing $E_{B(t)} \propto LE_{B(t)}t$ is a reasonable assumption made to predict battery life.

Combining our stored energy estimate with our lifespan prediction:

$$N = \frac{E_{B(t)}}{E_A} = \frac{E_{B0} + \varepsilon E_I \omega_I t - E_A \omega_A t}{E_A(1 + Lt)} = T\omega_A$$

$$T = \frac{E_{B0} + \varepsilon E_I \omega_I t - E_A \omega_A t}{E_A \omega_A (1 + Lt)}$$

$$T(1 + Lt) - t(\varepsilon E_I \omega_I - E_A \omega_A) = \frac{E_{B0}}{E_A \omega_A}$$

$$T + LTt - t(\varepsilon E_I \omega_I - E_A \omega_A) = \frac{E_{B0}}{E_A \omega_A}$$

setting $t = T$ to determine the maximum lifetime we see this a quadratic equation with constant coefficients.

$$LT^2 + T(1 - \varepsilon E_I \omega_I + E_A \omega_A) - \frac{E_{B0}}{E_A \omega_A} = 0$$

Solving for the maximum lifespan:

$$T = \frac{-(1 - \varepsilon E_I \omega_I + E_A \omega_A) \pm \sqrt{(1 - \varepsilon E_I \omega_I + E_A \omega_A)^2 + 4L \frac{E_{B0}}{E_A \omega_A}}}{2L}$$

Yielding the values

$$T = \frac{\varepsilon E_I \omega_I - (1 + E_A \omega_A)}{2L} + \frac{\sqrt{(1 - \varepsilon E_I \omega_I + E_A \omega_A)^2 + 4L \frac{E_{B0}}{E_A \omega_A}}}{2L}$$

and

$$T = \frac{\varepsilon E_I \omega_I - (1 + E_A \omega_A)}{2L} - \frac{\sqrt{(1 - \varepsilon E_I \omega_I + E_A \omega_A)^2 + 4L \frac{E_{B0}}{E_A \omega_A}}}{2L}$$

Where the first result is chosen as the lifespan cannot be negative.

The effect of each parameter E_A, ω_A, etc. can be studied by looking at the sensitivity of T to each one in turn. This is done by taking the partial derivative of T with respect of each parameter. Nominal values for each parameter are listed in Table 3-7. The sensitivity to each parameter is investigated in turn in the remainder of this chapter. For each sensitivity plot presented the remaining values are held constant at their stated nominal value. Sensitivity plots with different nominal values will be shifted or skewed relative to those presented here, but will maintain the same asymptotic features.

TABLE 3-7: DOOR STRIKE HARVESTER SYSTEM PARAMETERS

Term	Symbol	Units	Nominal Value
Initial battery energy	E_{B0}	Joules	9908
Current battery energy	$E_{B(t)}$	Joules	/
Input energy	E_I	Joules/input	0.564
Input frequency	ω_I	1/Month	800
Activation energy	E_A	Joules/activation	0.430
Activation frequency	ω_A	1/Month	300
Scavenging efficiency	ε	[/]	0.25
Activations remaining	N	#	/
Passive battery leakage	L	%/Month	0.02
Lifespan	T	Months	/

The sensitivity of harvesting efficiency, ε, on lifespan is given by:

$$\frac{\partial T}{\partial \varepsilon} = \frac{E_I \omega_I}{2L} - \frac{1}{2L} \frac{-E_I \omega_I (1 - \epsilon E_I \omega_I + E_A \omega_A)}{\sqrt{(1 - \epsilon E_I \omega_I + E_A \omega_A)^2 + 4LE_{B(0)}/E_A \omega_A}}$$

Its impact is plotted in Figure 3-3 with the remaining parameter values being those listed in Table 3-7.

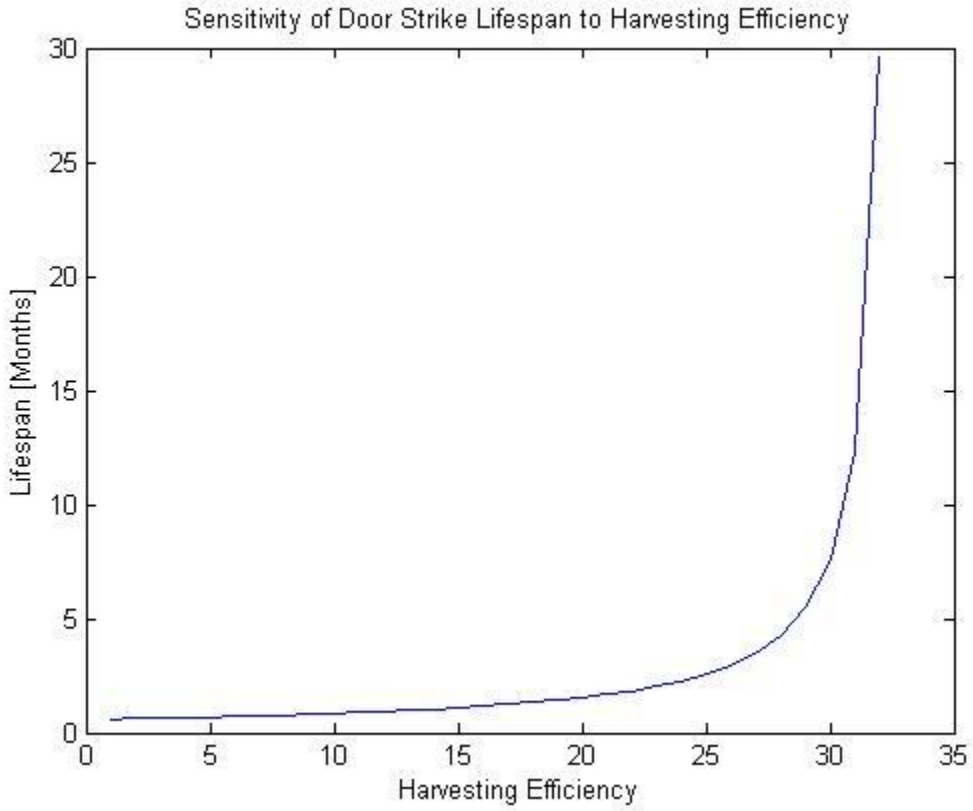

FIGURE 3-3: SENSITIVITY OF DOOR STRIKE LIFESPAN TO HARVESTING EFFICIENCY

The sensitivity to the initial battery capacity is given by:

$$\frac{\partial T}{\partial E_{B0}} = \frac{1}{E_A \omega_A} \frac{1}{\sqrt{(1 - \epsilon E_I \omega_I + E_A \omega_A)^2 + 4LE_{B(0)}/E_A \omega_A}}$$

Its impact is shown in Figure 3-4.

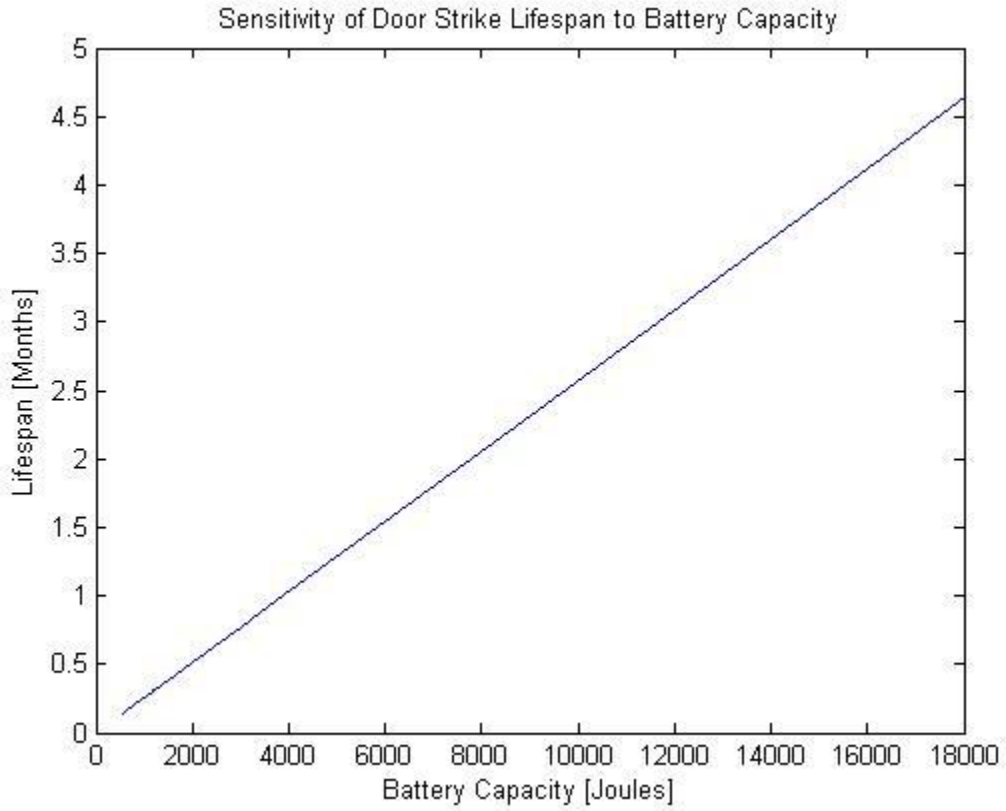

FIGURE 3-4: SENSITIVITY OF DOOR STRIKE LIFESPAN TO BATTERY CAPACITY

The sensitivity to input energy is given by:

$$\frac{\partial T}{\partial E_I} = \frac{\epsilon \omega_I}{2L} - \frac{\varepsilon \omega_I (1 - \epsilon E_I \omega_I + E_A \omega_A)}{2L\sqrt{(1 - \epsilon E_I \omega_I + E_A \omega_A)^2 + 4L E_{B(0)}/E_A \omega_A}}$$

And is shown in Figure 3-5.

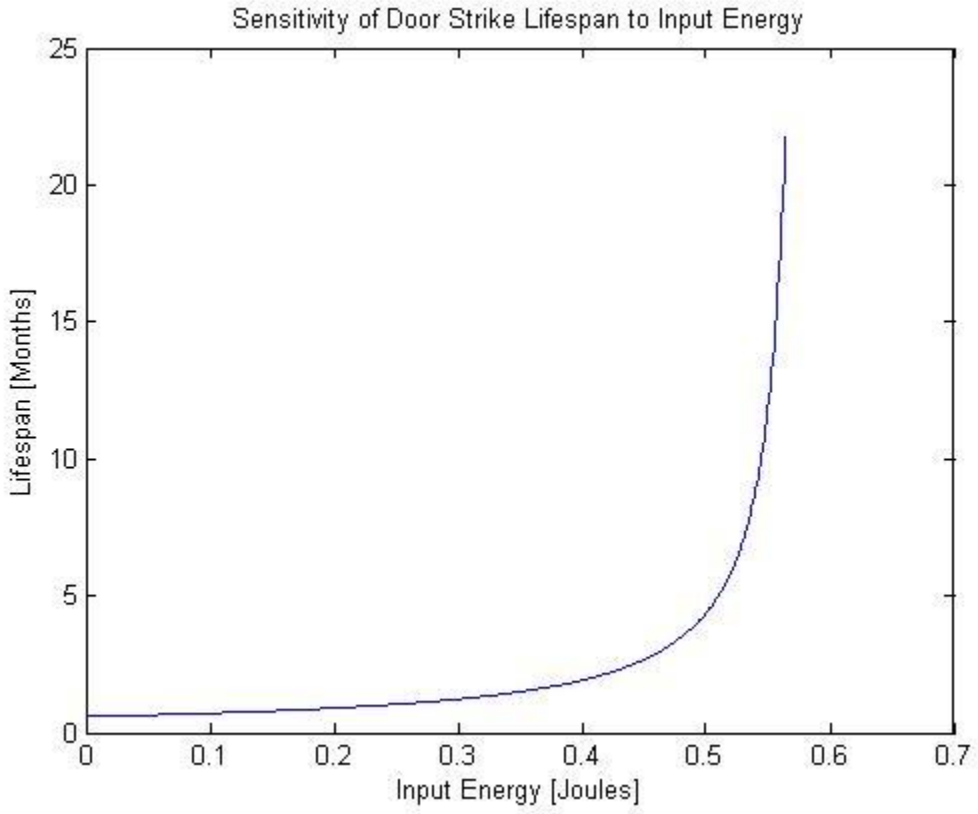

FIGURE 3-5: SENSITIVITY OF DOOR STRIKE LIFESPAN TO INPUT ENERGY

The sensitivity to activation energy is given by:

$$\frac{\partial T}{\partial E_A} = -\frac{\omega_A}{2L} - \frac{2\omega_A(1 - \epsilon E_I \omega_I + E_A \omega_A) - 4LE_{B0}/E_A^2 \omega_A}{4L\sqrt{(1 - \epsilon E_I \omega_I + E_A \omega_A)^2 + 4LE_{B0}/E_A \omega_A}}$$

And is shown in Figure 3-6.

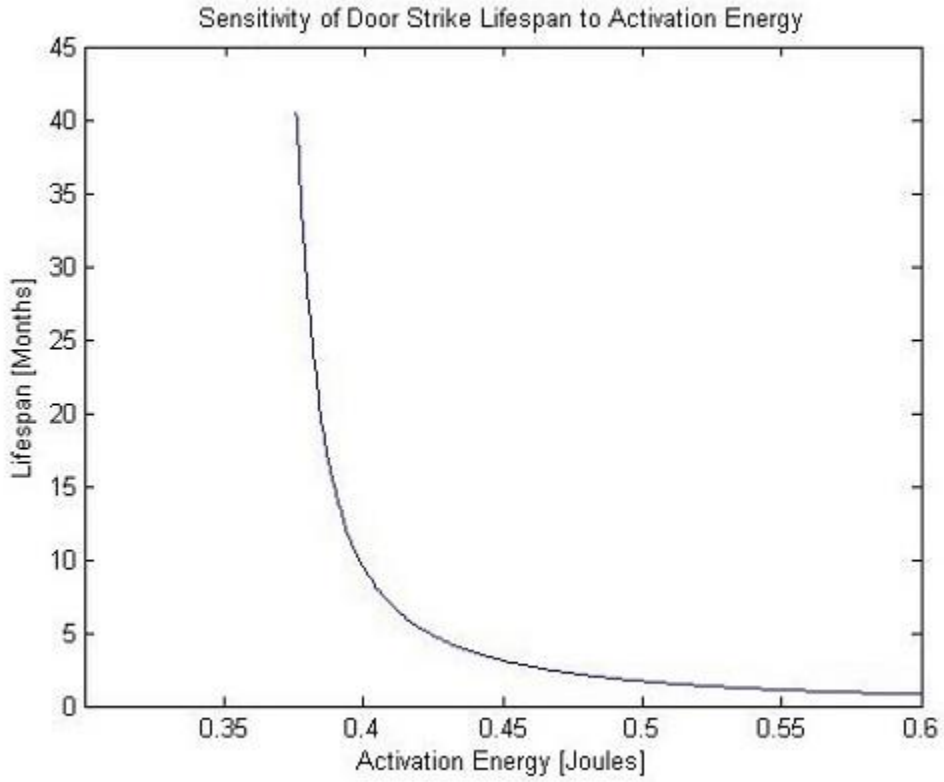

FIGURE 3-6: SENSITIVITY OF DOOR STRIKE LIFESPAN TO ACTIVATION ENERGY

The sensitivity of input frequency is given by:

$$\frac{\partial T}{\partial \omega_I} = \frac{\epsilon E_I}{2L} - \frac{\varepsilon E_I(1 - \epsilon E_I \omega_I + E_A \omega_A)}{2L\sqrt{(1 - \epsilon E_I \omega_I + E_A \omega_A)^2 + 4LE_{B(0)}/E_A \omega_A}}$$

And is shown in Figure 3-7.

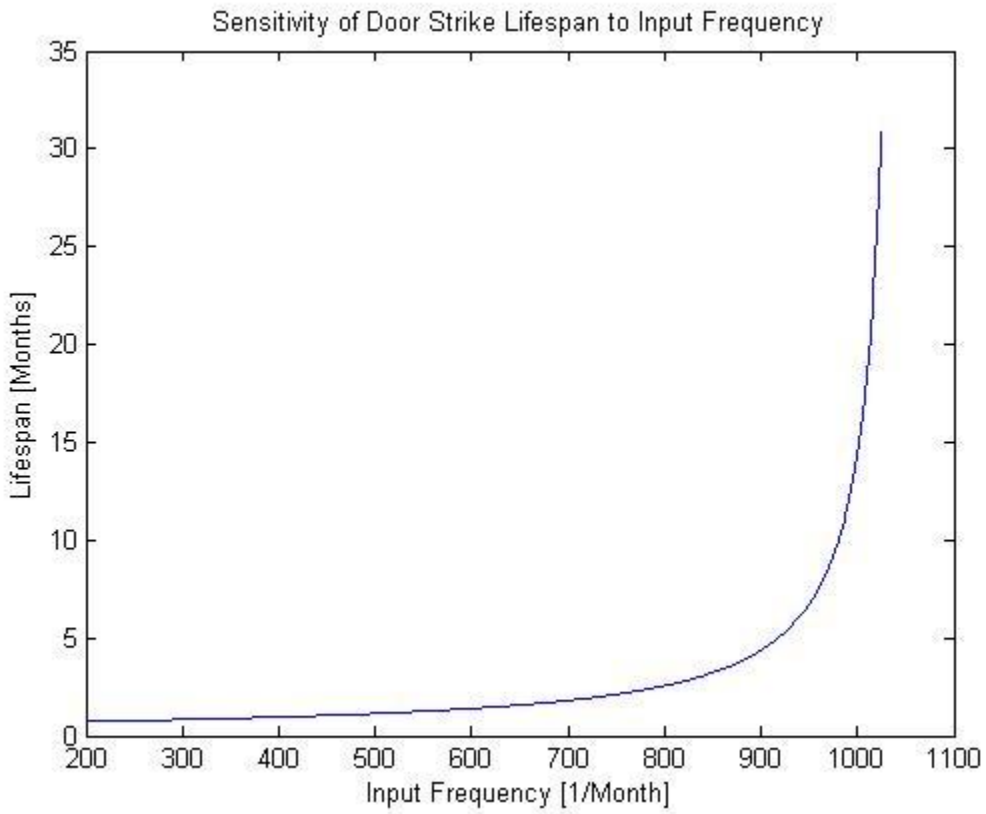

FIGURE 3-7: SENSITIVITY OF DOOR STRIKE LIFESPAN TO INPUT FREQUENCY

The sensitivity to activation frequency is given by:

$$\frac{\partial T}{\partial \omega_A} = -\frac{E_A}{2L} + \frac{2E_A(1 - \epsilon E_I \omega_I + E_A \omega_A) - 4LE_{B0}/E_A \omega_A^2}{4L\sqrt{(1 - \epsilon E_I \omega_I + E_A \omega_A)^2 + 4LE_{B(0)}/E_A \omega_A}}$$

And is shown in Figure 3-8.

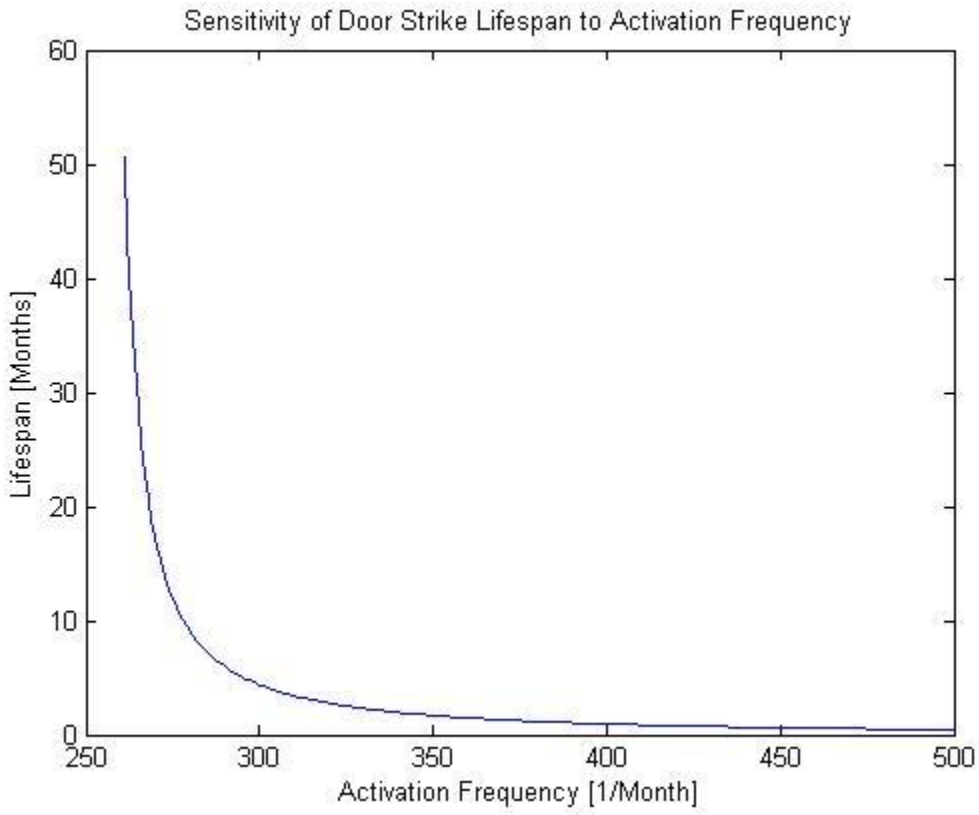

FIGURE 3-8: SENSITIVITY OF DOOR STRIKE LIFESPAN TO ACTIVATION FREQUENCY

The sensitivity to self-discharge rate, also called passive battery leakage, is given by:

$$\frac{\partial T}{\partial L} = \frac{(1 - \epsilon E_I \omega_I + E_A \omega_A)}{2L^2} - \frac{\sqrt{(1 - \epsilon E_I \omega_I + E_A \omega_A)^2 + 4LE_{B(0)}/E_A \omega_A}}{4L^2} + \frac{2E_{B0}}{\sqrt{(1 - \epsilon E_I \omega_I + E_A \omega_A)^2 + \frac{4LE_{B(0)}}{E_A \omega_A}}}$$

And is shown in Figure 3-9.

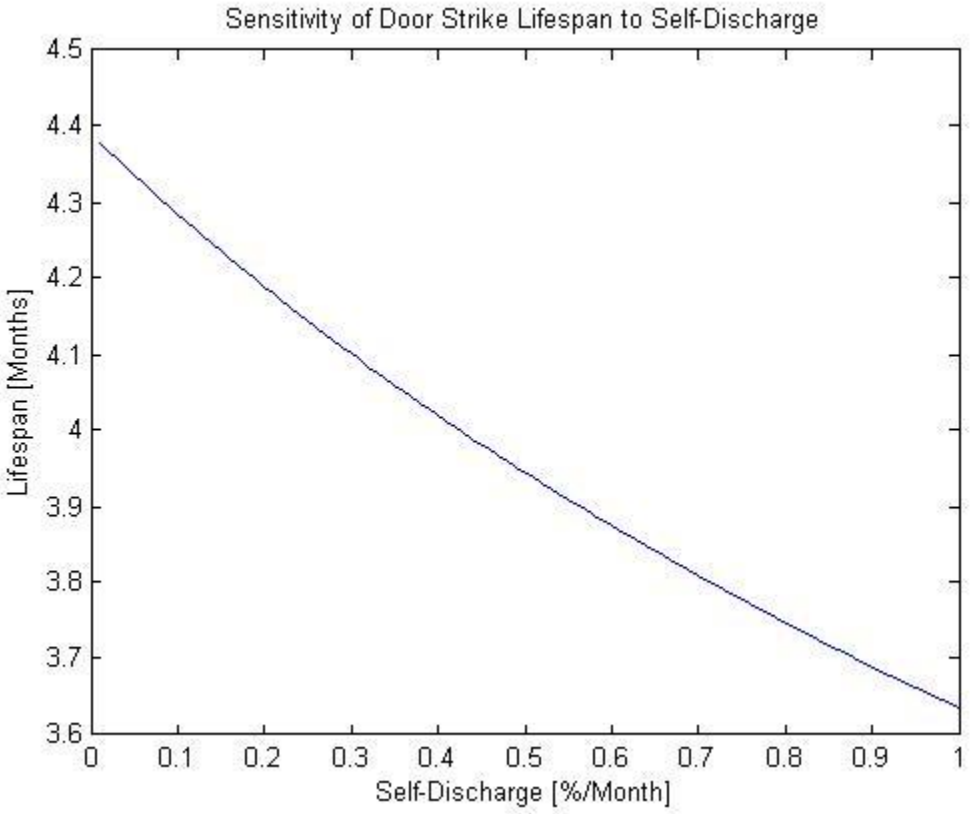

FIGURE 3-9: SENSITIVITY OF DOOR STRIKE LIFESPAN TO PASSIVE BATTERY LEAKAGE

Each parameter sensitivity can be thought of as a relative weight, with a higher weight having a greater impact on the system lifespan. Each parameter sensitivity shows a monotonically increasing or decreasing relationship to system life span. This property is true regardless of the remaining parameter values, which indicates that each may be either maximized or minimized independently, without the need to involve complex interaction models.

While the general trend of each sensitivity curve is not particularly surprising (i.e. increasing efficiency or energy input always increases lifespan) The relative impact of each parameter is important to know when design requirements necessitate making a choice between two or more parameters.

Now that a conceptual framework for battery lifespan has been identified we can quantify the individual parameter values, specifically the input energy, activation energy, and harvesting efficiency.

4. DOOR STRIKE HARVESTER

4.1.DOOR STRIKE ENERGY FLOW

The detailed design of the E-strike can begin by arriving at an estimate of the maximum available energy. The International Code Council states that the maximum force necessary to open a door should not exceed 5 Lbf (22.2N) for an interior door, and 15Lbf (66.7N) for a fire exit [36]. It is assumed that the resistive force exerted by the latch of the door strike is equal to this maximum value of 22.2N. A typical strike plate will have a width of approximately 1" (25.4mm). Assuming a nearly constant force is applied over this distance the maximum allowable input energy into the strike will be:

$$E_{in} = Force \times Distance = 22.2N \times 0.0254m = 0.564\,J$$

This maximum value may not be available in practice as mechanical designs and further limitations on the strike latch force will exist. A more reasonable estimate of the upper limit of attainable input energy is taken to be ~90% of this value or 500mJ.

It must be considered how this energy enters the system. As the latch is displaced it must have a return spring that resists the input force. it will initially absorb and then return a portion of this energy. The reaction torque on the latch is then a summation of the generator resistive torque and spring torque. As the spring torque must be great enough to overcome the generator resistive torque to return the latch to its initial position we have the requirement that $k\Delta\theta \geq T_{gen},\ \theta \neq 0$, during the return motion. The generator torque is not constant, but instead is a function of the speed at which the latch is rotated. this speed will be assumed to be both constant over the full range of motion and consistent across activations. While it is simple to substantially increase the spring stiffness to ensure this inequality, doing so would result in increased energy losses as the excess stored spring energy would dissipate upon latch return rather than be taken in by the generator. The energy flow through the system is conceptually depicted in Figure 4-1.

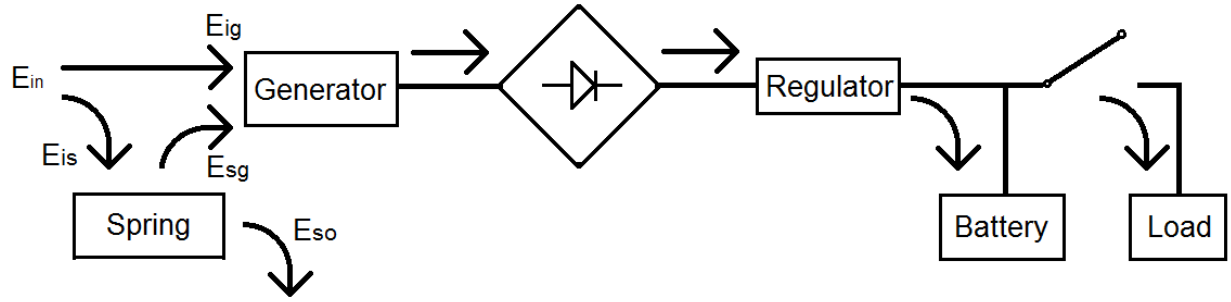

FIGURE 4-1: ENERGY FLOW DIAGRAM OF HYBRID E-STRIKE

$$E_{in} = E_{is} + E_{ig} = \frac{1}{2}k\theta^2 + \int T_{Gen} \cdot \omega \, dt$$

$$E_{is} = E_{so} + E_{sg} = E_{so} + \int T_{Gen} \cdot \omega \, dt$$

As E_{so} represents an energy loss term the maximum input efficiency will exist when $E_{so} = 0$ which leads to $E_{in} = \frac{1}{2}k\theta^2 + \int T_{Gen} \cdot \omega \, dt$. The generator resistive torque, T_{Gen}, is dependent upon the generator parameters, specifically the torque constant and rotor inertia.

The analysis in Chapter 3 showed clear relationships between each system parameter and E-strike longevity. In all cases the relationship is either monotonically increasing or decreasing and this hold true regardless of the remaining parameter values. Any optimization study of an E-strike will result in the simple case of maximization or minimization of each value, independent of all the remaining terms. This chapter will focus on establishing baseline values for each parameter and in so doing, identify under what operating conditions an E-strike will be able to operate successfully.

4.2.SUBSYSTEM EXPERIMENTS

the E-strike test apparatus is divided into 4 main components; the rotational generator & corresponding gear assembly, the bridge rectifier & regulator (referred to as the energy harvesting electronics, or EHE), the battery, and the locking circuitry or load. For the generator there is an associated input energy and conversion efficiency, The EHE also has some energy losses which will be modelled as a transfer efficiency. The battery and recharging circuit will likewise have some losses. Lastly the load will have a required activation energy. These sub components will be first tested individually to identify their corresponding values and from there an amalgamated overall efficiency will be determined.

Looking first at the generator & gearing the nominal efficiency value can be taken as an initial estimate. This efficiency value is velocity dependent, which is controllable through the gear ratio. fundamentally, the input velocity at the latch is uncontrollable, but will be assumed to be consistent across each discrete door opening. For this analysis it is taken to be 7.85 rad/s, and labelled ω_L. The generator shaft is directly connected to the latch via multistage gear reduction, which modifies both the latch torque, T_L, and latch speed, ω_L. The energy across the gear set and into the generator can be expressed as:

$$\int_0^t T_L \cdot \omega_L dt = \int_0^t T_{gen} \cdot \omega_{gen} dt$$

Where the corresponding gear ratio, 'n', between the latch and generator is:

$$n = -\frac{\omega_{gen}}{\omega_L}$$

The negative sine accounts for the change in rotational direction between input gear and pinion. For our purposes this detail may be disregarded and the absolute value of the gear ratio will be the point of interest. The generator reaction torque and corresponding current produced are given by:

$$T_{gen} = F_{(\omega_{gen})} = J\ddot{\theta} + K\theta + k_t i$$

$$L\dot{i} + Ri + k_t\theta = 0$$

Where 'ki' is the generator constant with dimensions $[Nm/A] \equiv [V/rad/s]$. The current, 'i', out of the generator is a complex function due to the EHE circuitry. The generator used is a Maxon Motor DCX 22L mm , with torque constant and rotor inertia of 6.95 mNm/A, and 9.67 g•cm^2 including gearbox, respectively. Taking the Laplace transform of these two equations to obtain the transfer function between theta and the reaction torque:

$$\frac{T_{(s)}}{\theta_{(s)}} = Js^2 + K - \frac{k_T^2 s}{Ls + R}$$

For a constant angular velocity, $\dot{\theta}$, $\theta_{(s)} = \omega_{gen}/s^2$, the torque equation becomes:

$$T_{(s)} = \frac{\omega_{gen}}{s^2}(Js^2 + K - \frac{k_T^2 s}{Ls + R})$$

The inverse Laplace is then:

$$T_{(t)} = \omega_{gen}(\frac{k_T^2 e^{\frac{-Rt}{L}}}{R} - \frac{k_T^2}{R} + J\delta_{(t)} + Kt)$$

For typical generator parameter values this expression will be dominated by the spring stiffness, K, and shaft velocity, ω_{gen}. With the generator efficiency being a function of shaft velocity, and since this velocity is coupled to the input latch velocity and torque there arises the situation where maximum

harvested energy may not occur at the generator's optimal operating speed. The maximum input torque allowable is governed by [36] discussed earlier, and to a small extent the mechanical design of the latch. This maximum torque value is approximately $320\ mNm$, with an input velocity of 7.85 rad/s. The generator reaction torque must then be less than $n \cdot T_L$.

Accounting for the conversion efficiency the electrical energy harvested is:

$$E_{electrical} = \int_0^t \varepsilon_{gen}(\omega) \cdot T_{gen}(\omega) \cdot \omega_{gen} dt$$

Both $\varepsilon_{gen}(\omega)$ and $T_{gen}(\omega)$ are functions of the gear ratio, n, given that the input velocity is known and constant. Electrical energy is then a function of the controllable gear ratio value. Harvested electrical energy for different gear ratios is presented in Table 4-1.

TABLE 4-1: ELECTRICAL ENERGY FROM THE GENERATOR FOR DIFFERENT GEAR RATIOS

Input Energy [mJ]	Gear Ratio, n [output/input]		Energy harvested [mJ]	Generator efficiency, ε []
113.5	22		7.66	6.75
152.3	29.3		22.01	14.45
162.6	33		29.59	18.2
159.8	35.2		31.93	19.98
206.1	44		46.62	22.62
294.1	55		76.67	26.07
341.1	58.7		109.62	32.11
379.3	66		124.1	32.72
501.2	88		200.95	40.1

The maximum energy is obtained with an gear ratio of 88:1, which will be used in all subsequent experiments. The generator is then operating at an efficiency of 40.1 %.

Evaluation of the EHE efficiency is done in tandem with the generator by measuring the voltage and current across the generator leads that connect to the EHE. This allows for calculation of the electrical input energy. The electrical output is regulated to 3.6V and discharged through a 470 ohm resistor. Efficiency values of the EHE for various input energies are presented in Table 4-2.

TABLE 4-2: EHE ELECTRICAL CONVERSION EFFICIENCIES

Electrical Input Energy [mJ]	Rectified & Regulated Energy [mJ]	Efficiency []
139.3	92.0	0.66
142.3	87.8	0.62
143.4	93.9	0.65
147.2	92.0	0.62
155.5	100.5	0.65
162.2	109.9	0.68
168.5	106.2	0.63
196.6	128.0	0.64
224.1	136.4	0.61

The EHE has a fairly consistent efficiency within the range of energy levels tested, with an average of 64%. This value is combined with our peak generator efficiency of 40.1% to get an overall harvesting efficiency estimate of 0.401*0.64=0.26, or 26%. This value, along with the input energy, activation energy, initial battery capacity, and passive leakage, will be applied in our model from Section 3 to arrive at an estimate of system lifespan to be compared to experimental results.

The locking circuitry is tested to identify the necessary energy needed to activate the radio receiver, timing circuit and micro motor. The load schematic is presented in Figure 4-2.

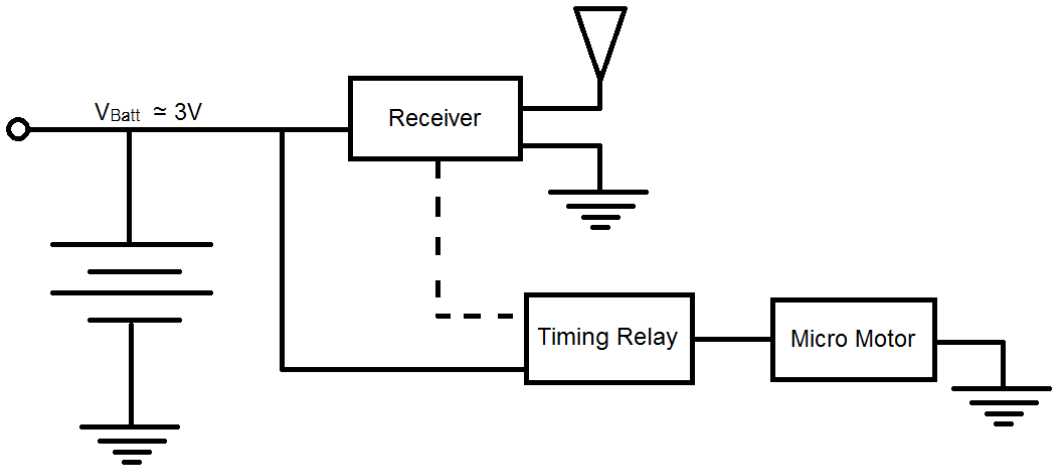

FIGURE 4-2: LOAD CIRCUITRY OPERATING AT 3 VOLT LOGIC

On each activation the load is powered for 4.5 seconds and is found to consume approximately 430 mJ. This value is set to be our activation energy, E_A.

Testing of the battery is considerably more complex as there are no concise models that describes battery voltage, stored charge, passive discharge, and recharging performance. an analysis will be done on the complete system instead.

4.3. FULL SYSTEM EXPERIMENTS

To determine the feasibility of this hybrid design concept the mock door strike depicted below was fabricated. It allows for the interchanging of gears and return springs to investigate their effect, as well as a standard rectification and storage circuit. The output of this circuitry is regulated to 3.6V and is used to recharge the battery as well as partially power the locking circuitry.

As discussed previously, the two primary uncontrollable operating parameters within the door strike are the activation frequency and energy input frequency, or how often the door is locked/unlocked and how often it is opened, respectively. Together these two values describe the rate of energy consumption and the rate of energy put into the system. The ratio of activation frequency and input frequency, hence referred to as the A/I ratio, can be seen as a normalizing parameter that characterizes the environment the E-strike will operate in. While door usage rates will not be constant over a full day or full work week, average rates of input and activation over long periods of time can be assumed to be constant. As it is assumed the door will never be locked/unlocked without a corresponding opening this ratio is bounded between 0 and 1.0, with 0 referring to cases where the door is opened and closed, but never locked. An A/I ratio of 1.0 is the worst case scenario in terms of energy consumption as the locking circuitry will activate upon every door opening. Experiments described in this section were performed to identify the maximum A/I ratio attainable based on the overall system performance, accounting for generator efficiency, rectification & regulation, and battery recharging efficiency. The full experimental system schematic is shown in Figure 4-3.

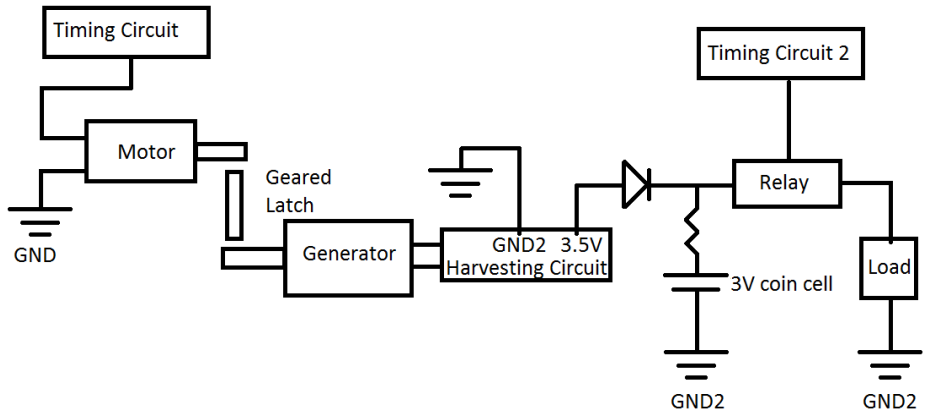

FIGURE 4-3: HYBRID DOOR STRIKE EXPERIMENTAL DIAGRAM

The energy harvester located within the door strike will be a rotational electromagnetic generator as described. As before it will harvest energy from latch motion and this electrical energy will be rectified and regulated. The locking circuitry, consisting of a radio receiver, timing circuit and micro motor, will be activated for 4.5 seconds and dissipate approximately 430 mJ each cycle. The experimental prototype is shown below. A larger motor will act as a stand-in for a human operator to engage the latch.

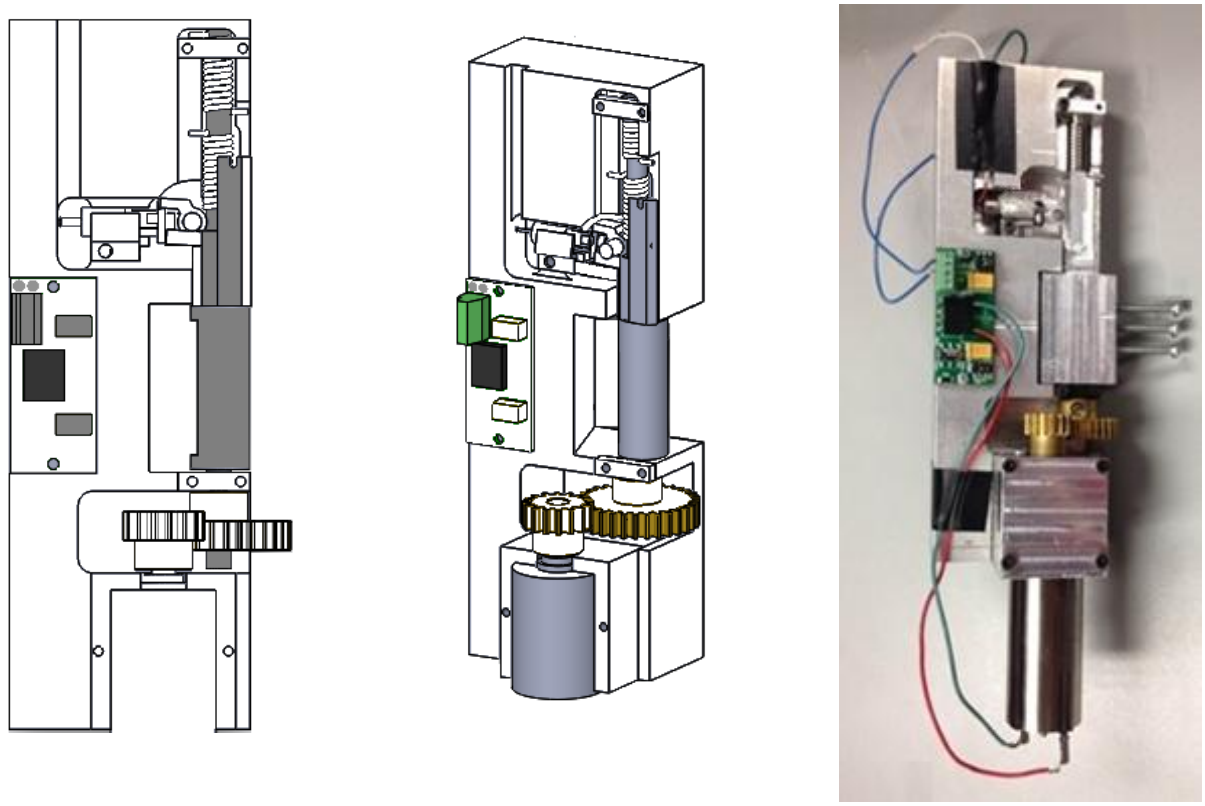

FIGURE 4-4: E-STRIKE TESTING APPARATUS

The battery used is a vanadium Pentoxide lithium ion coin cell. It has a nominal voltage of 3V, a capacity of 100mAh (108000 mJ), and is rated for approximately 1000 recharge cycles at 10% discharge capacity. For each trial a new coin cell was connected to the system and the activation A/I ratio was varied by changing the activation frequency. As a benchmark, Trial 1 tested an A/I ratio of infinity, i.e. the battery supplies all of the energy and no harvesting circuit is connected.

Voltage readings of the coin cell and load were taken periodically. From these values we can determine the charge flow through the strike system. The load voltage is measured prior to the relay and so is a measure of the recharging voltage when its value is above that of the battery. It is equal to the battery voltage when the relay is disengaged.

The charge into the battery is given by:

$$\frac{V_{Load} - V_{Bat}}{R} = \dot{q}_{in}$$

which suggests that as the battery charge decreases the recharging perforance, $\dot{q}_{in}$, improves. Likewise during discharge the charge exiting the battery is:

$$\dot{q}_{out} = \frac{V_{Bat}}{R + R_{Load}}$$

This suggests there may exist equilibrium points at battery voltages below $V_{B(0)}$ where the net charge through the battery over time is zero. If we also consider that the voltage at the output of the EHE, V_{EHE}, is not zero during activation time, the charge out of the battery will be slightly less than $\dot{q}_{out}$ as some charge will flow directly from the EHE to the load and bypass the battery entirely.

To determine hybrid battery lifetime the testing apparatus is repeatedly activated and recharged with a given A/I ratio until failure, which is defined as when the battery voltage falls and remains below 2.5V. The number of activations performed prior to failure is recorded as the lifespan of the system operating at that specific A/I ratio.

For lower A/I ratios - in the range of 0.1 to 0.01 - the simulation predicts an infinite lifespan as the total input energy exceeds the output energy over a sufficient time span. This means there is a 'break even' A/I ratio where the input and output energies balance. This can be calculated as follows:

$$Total\ energy\ in = E_{in} \times N_{in} \times \varepsilon$$

$$Total\ energy\ out = E_A \times N_A$$

where E is the energy into or out of the system, N is the number of inputs or activations, and Ɛ is the total system harvesting efficiency. Setting these two energy flows to be equal and rearranging the terms we can solve for the maximum A/I ratio that could theoretically have an infinite lifespan.

$$\frac{A}{I} ratio = \frac{N_A}{N_{in}} = \frac{\varepsilon E_{in}}{E_A}$$

Assuming the following values for E_{in}, E_A, and Ɛ of 500mJ, 430mJ, and 0.15, respectively the maximum theoretical A/I ratio given current findings is equal to 0.17. Note this simplified calculation does not

consider battery degradation, or passive current leakage, both factors will reduce the attainable A/I in practice. As there are multiple factors than potentially impact the attainable A/I ratio calculated predictions are compared to experimental values. Hybrid system lifespans for different A/I ratios are presented in Table 4-3. These values are contrasted to the analytically predicted values based on the model presented in the previous section.

TABLE 4-3: HYBRID E-STRIKE LIFESPANS BASED ON A/I RATIO

A/I Ratio		Predicted Lifespan (# Activations)	Recorded Lifespan (# Activations)
Infinite		1006	999
1		1372	5630
0.5		2123	9990
0.2		24250	23820
0.1		>100 000	Indefinite
0.02		>100 000	indefinite

Battery charge as a function of the number of activations are presented below for sample experimental cases.

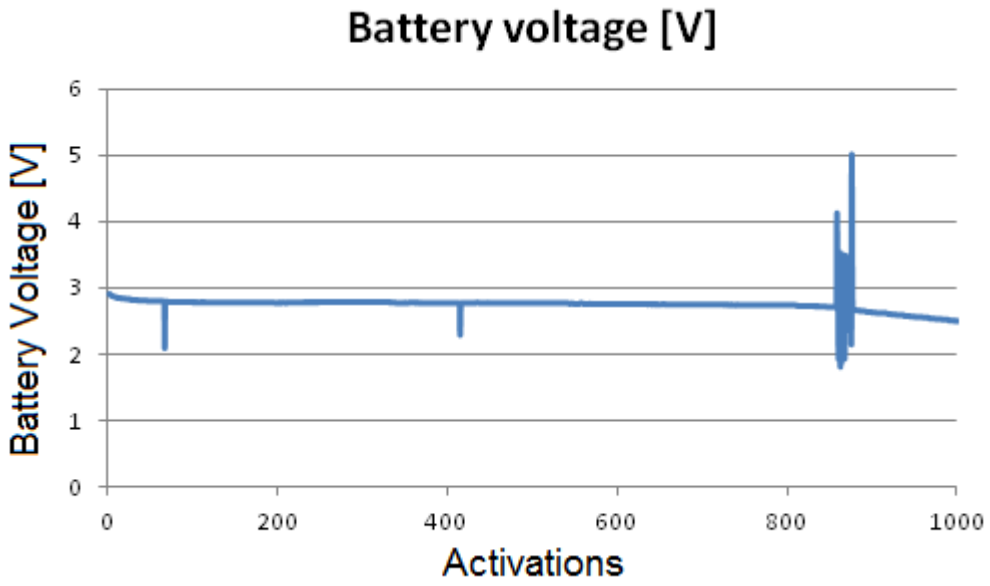

FIGURE 4-5: BATTERY VOLTAGE DROP FOR AN A/I RATIO OF INFINITY (NO HARVESTING)

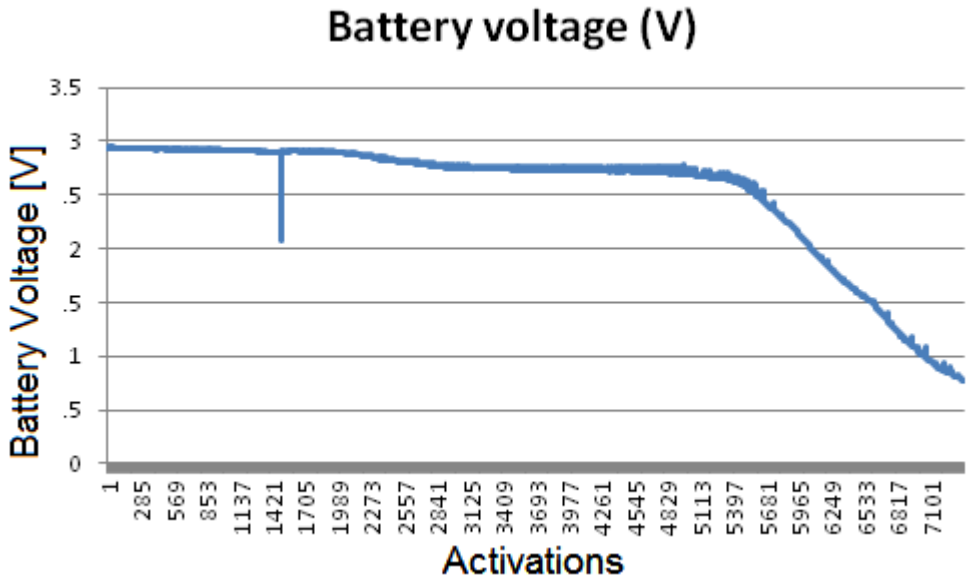

FIGURE 4-6: BATTERY VOLTAGE DROP FOR AN A/I RATIO OF 1.0

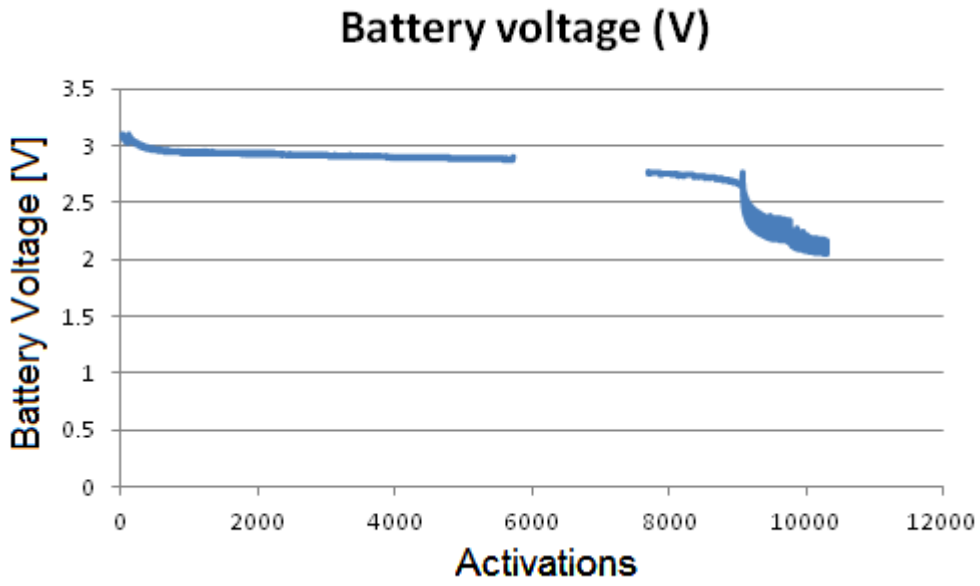

Figure 4-7: Battery Voltage Drop for an A/I Ratio of 0.5

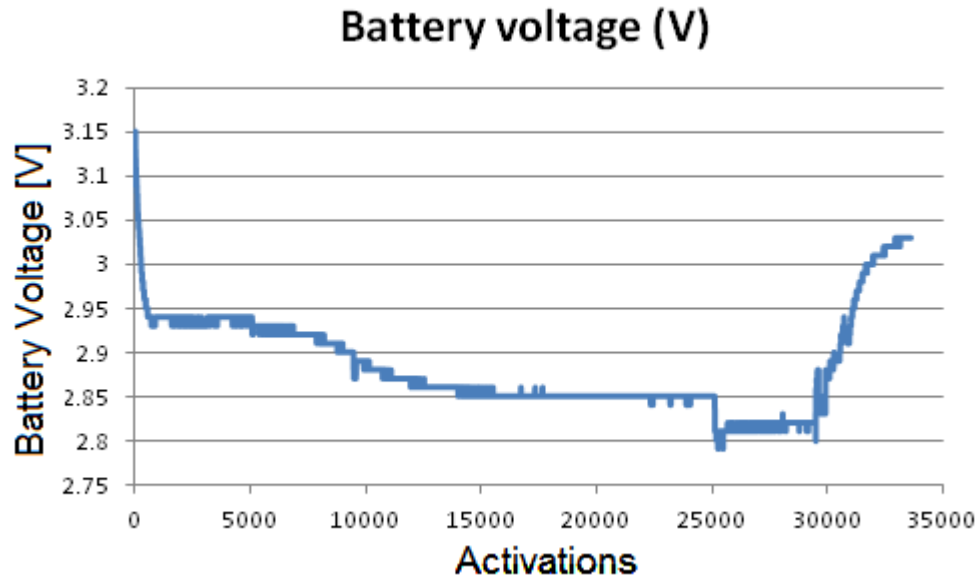

FIGURE 4-8: BATTERY VOLTAGE DROP FOR AN A/I RATIO OF 0.1

4.4.DISCUSSION

Comparisons between experimental and simulated results must be qualified. First, as these experiments were conducted over the course of days or weeks depending on the trial, rather than months, passive leakage was not measured effectively, which would inflate experimental life spans. Furthermore, this simulation assumes all energy can be extracted from a battery, when in reality once the battery voltage drops below a usable level - here defined as 2.5V - it is effectively dead as it will be unable to operate the necessary circuitry, though still possessing potential energy, inflating simulated life spans.

Experiments show that a net positive energy flow into the storage battery exists at an A/I ratio of 0.1 or below. With an activation energy of 430 mJ and a mechanical input energy of 250 mJ this leads to an average total efficiency of 17%. This is below the previously estimated efficiency of 26% noted in Section 4.2, which is expected as it also accounts for the battery recharging efficiency that was previously unknown.

It was noticed during the experiments that the harvesting efficiency is highly sensitive to latch speed, due primarily to the generator's efficiency being coupled to its shaft speed. This is most evident in the experimental results in Trial 4, with an A/I ratio of 0.1. After approximately 30000 activations the apparatus was adjusted slightly to correct mechanical stiction present due to wearing of the latch bushing surface. the input motor power was increased slightly (from 12V to 12.2V), leading to a minor increase in input latch velocity. this adjustment was later discovered to be significant enough to transition the system from operating with a small net negative energy loss to a positive net energy flow, and therefore an indefinite lifespan. Latch velocity is clearly a highly significant factor in system performance as it directly controls the generator shaft velocity, but remains an uncontrollable parameter within the present design.

Despite the highly sensitive efficiency of the prototype system the feasibility of a hybrid E-strike system with a net positive energy flow, and therefore an indefinite lifespan, has been demonstrated. Any A/I ratio below 0.1 will then also have an indefinite lifespan.

5. CONCLUSION

Energy sources suitable for use with an E-strike have been identified and their power densities quantified from values reported in the literature. Multiple different conversion methods have been investigated. It was concluded that a rotational electromagnetic generator is the most suitable conversion method. It's operation as a harvester has been quantified, both as a standalone electric generator, when paired with electrical rectification and regulation circuitry, and as a complete E-strike including battery recharging and locking circuitry. This full E-strike prototype has been assembled and investigated to quantify the analytical model derived in Section 3.4. Experimentally determined lifespans are compared to analytical predictions and there is approximate agreement between the model and measured data. A number of sources of error have been identified and discussed.

These experiments were performed under highly controlled conditions. The motor used to engage the strike provides a highly uniform velocity input, whereas human operators are unlikely to be as consistent. Human operators are expected to open the door with slightly higher velocities, thereby operating at a higher generator efficiency. The sensitivity to latch velocity is most apparent in Figure 4-8 where adjustment of the testing apparatus at the 30000 cycle mark slightly increased the applied torque and hence the latch velocity. This minor change in velocity is sufficient enough to transition the system from a slow net loss in energy to a rather significant net gain in stored energy over time, which corresponds to an infinite operation lifespan.

This sensitivity leads to variability in predicting harvesting efficiency as the rotational generator efficiency is velocity dependent. The generator voltage is also a function of latch velocity and this voltage directly impacts the rectification and regulation circuitry in a manner that is difficult to quantify due to the nonlinear nature of the electronics. In general, a higher velocity will lead to increased generator efficiency, greater voltages, and improved rectification performance.

A constant input frequency produced by the timing circuit is also unrealistic as door operation is expected to occur in clusters during peak times of the day (morning, noon, end of work day), rather than evenly spread out. This factor is important to keep in mind as our experiment provides more uniform battery charging conditions, which is a significant factor in battery lifetime. Uniform activation rate is also a significant factor effecting battery lifetime as it contributes to the maximum number of charge/discharge cycles a battery can undergo, as well as the depth of discharge a battery experiences.

This study is successful in demonstrating the existence of a indefinite E-strike operational lifespan under certain operating conditions. Refinement of the prototype design with emphasis based upon the criteria identified in Section 3.4 will improve operation across all environments. The decision as to whether or not a hybrid E-strike will be suitable to operate within a specific environment can be made based primarily upon a single derived factor, which is the expected A/I ratio it will experience in that environment.

The simplified calculations used to derive the maximum currently attainable A/I ratio show promising results as there are many scenarios where a door will be opened far more often than it is (un)locked. Simulations that consider additional factors such as passive leakage current also suggest there exists a smaller, but significant A/I ratio that will lead to an infinite system lifespan. While a truly infinite lifespan

is unattainable due to physical wear and battery degradation, a system that lasts several hundred thousand activations may yet be feasible.

7. REFERENCES

[1] "Kickstarter/evolved charger," 20 August 2015. [Online]. Available: https://www.kickstarter.com/projects/evolvedcharger/usbidi-the-worlds-most-intelligent-charger-ever?ref=category_popular.

[2] "Kickstarter/mix stik," 20 August 2015. [Online]. Available: https://www.kickstarter.com/projects/1614456084/mixstik-the-magic-stick-to-mix-perfect-cocktails?ref=category.

[3] "Kickstarter/smart 2 move," 20 August 2015. [Online]. Available: https://www.kickstarter.com/projects/smart2move/smartbalance-light-made-to-improve-your-balance-an?ref=category.

[4] C.-X. Zu and H. Li, "Thermodynamic analysis on energy densities of batteries," *Energy & Environmental Science,* vol. 4, pp. 2614-2624, 2011.

[5] E. Cantatore and M. Ouwerkerk, "Energy scavenging and power management in networks of autonomous microsensors," *Microelectronics,* pp. 1584-1590, 2006.

[6] S. Li, J. Yuan and H. Lipson, "Ambient wind energy harvesting using cross-flow fluttering," *Journal of Applied Physics,* vol. 109, no. 2, 2011.

[7] C. Mathuna, T. O'Donnell, R. Marinez-Catala and J. O. B. Rohan, "Energy scavenging for long-term deployable wireless sensor networks," *Remote Sensinng: Special Section,* pp. 613-623, 2008.

[8] Y. C. Shu and I. C. Lien, "Analysis of power outputs for piezoelectric energy harvesting systems," *Smart Materials and Structures,* vol. 15, pp. 1499-1502, 2006.

[9] E. Lefeuvre, A. Badel, C. Richard, L. Petit and D. Guyomar, "A comparison between several vibration-powered piezoelectric generators for standalone systems," *Sensors and Actuators,* vol. 126, no. 2, pp. 405 - 416, 2006.

[10] M. Lallart, C. Richard, L. Garbuio, L. Petit and D. Guyomar, "High efficiency, wide load bandwidth piezoelectric energy scavenging by a hybrid nonlinear approach," *Sensors and Actuators A: Physical,* vol. 165, pp. 294 - 302, 2011.

[11] D. Guyomar, A. Badel, E. Lefeuvre and C. Richard, "Toward Energy Harvesting Using Active Materials and Conversion Improvement by Nnlinear Processing," *Transactions on Ultrasonincs, Ferroelectrics, and Frequency Control,* vol. 52, no. 4, pp. 584 - 595, 2005.

[12] S. Shahruz, "Design of mechanical band-pass filters with large frequency bands for energy scavenging," *Mechatronics,* pp. 523-531, 2006.

[13] V. Challa, M. Prasad, Y. Shi and F. Fisher, "A vibration energy harvesting device with bidirectional

resonance frequency tunability," *Journal of Smart Materials and Structures,* 2008.

[14] J. Ward and S. Behrens, "Adaptive learning algorithms for vibration energy harvesting," *Journal of Smart Materials and Structures,* vol. 17, no. 3, 2008.

[15] J. Scruggs, "An optimal stochastic control theory for distributed energy harvesting methods," *Journal of Sound and Vibration,* vol. 320, pp. 707-725, 2009.

[16] S. Roundy, P. Wright and J. Rabaey, Energy scavenging for wireless sensor networks: with special focus on vibrations, Boston: Kluwer Academic Publishers, 2004.

[17] J. Thomas, M. Qidwai and J. Kellogg, "Energy scavenging for small-scale unmanned systems," *Journal of Power Sources,* pp. 1494-1509, 2006.

[18] J. Wang, T. Lin and L. Zuo, "High efficiency electromagnetic energy harvester for railroad application," in *ASME 2013 International Design Engineering Technical Conferences and Computers and Information in Engineering Conference*, Portland, Oregon, 2013.

[19] "Energy Harvesting Generators," Cherry, [Online]. Available: http://cherryswitches.com/product/energy-harvesting-generators/. [Accessed 16 December 2015].

[20] Panasonic, "Vanadium rechargable lithium batteries (VL series)," Panasonic, 2006.

[21] I. Buchmann, "Battery University - Elevating self discharge," Coalescent Design, 18 June 2015. [Online]. Available: http://batteryuniversity.com/learn/article/elevating_self_discharge. [Accessed 15 August 2015].

[22] I. Buchmann, "Battery University - How to define battery life," Coalescent Design, 18 June 2015. [Online]. Available: http://batteryuniversity.com/learn/article/how_to_define_battery_life. [Accessed 16 August 2015].

[23] J. Paradiso and T. Starner, "Energy scavenging for mobile and wireless electronics," *Pervasive Computing volume 4 issue 1,* pp. 18-27, 2005.

[24] J. Matiko, N. Grabham, S. Beeby and M. Tudor, "Review of the application of energy harvesting in buildings," *Measurement Science and Technology,* pp. 12002-12027, 2013.

[25] "Introduction to Solar Radiation," Newport Corporation, October 2013. [Online]. Available: http://www.newport.com/Introduction-to-Solar-Radiation/411919/1033/content.aspx. [Accessed February 2016].

[26] J. Gilbert and F. Balouchi, "A vibrating cantilever footfall energy harvesting device," *Journal of Intelligent Systems and Structures,* pp. 1738-1745, 2014.

[27] Mide Technologies, "Mide Energy Harvesting Electronics," 23 January 2013. [Online]. Available: http://www.mide.com/pdfs/volture_EHE004_Datasheet.pdf. [Accessed 23 May 2014].

[28] R. Cordero, A. Rivera, M. Neuman, R. Warrington and E. Romero, "Micro-rotational electromagnetic generator for high speed applications," in *Micro Electro Mechanical Systems (MEMS)*, Paris, France, 2012.

[29] E. Aktakka, H. Kim and K. Najafi, "Energy scavenging from insect flight," *Journal of Micromechanics and Microengineering,* 2011.

[30] T. Toh, P. Mitcheson and E. Yeatman, "A gravitational torqu micro-generator for self-powered sensing," in *Proceedings of Micromechanics Europe*, Guimaraes, Portugal, 2007.

[31] I. Paprotny, S. Sanders and P. Wright, "Broadband energy scavenging from vibrations using an eccentric rotor electromagnetic generator," in *PowerMEMS*, Atlanta, Georgia, 2012.

[32] C. Pylatiuk, F. Metzger, R. Wiegand and G. Bretthauer, "Kinetic energy scavenging in a prosthetic foot using a fluidic system," *Biomedical Technology,* pp. 353-358, 2013.

[33] T. Starner and J. Paradiso, "Human generated power for mobile electronics," in *Low power electronics design*, New York, CRC Press, 2004.

[34] "Ask a Mathematicion / Ask a Physicist," July 2010. [Online]. Available: http://www.askamathematician.com/2010/07/q-whats-the-chance-of-getting-a-run-of-k-successes-in-n-bernoulli-trials-why-use-approximations-when-the-exact-answer-is-known/. [Accessed 30 November 2015].

[35] "Battery performance characteristics - how to specify and test a battery," Woodbank Communications Ltd., 2005. [Online]. Available: http://www.mpoweruk.com/performance.htm. [Accessed 1 August 2015].

[36] Internaltional Code Council, "Public Building Code," International Code Council, 2007.

[37] L. Du, G. Shi and J. Zhao, "Review of micro magnetic generator," *Sensors & Transducers,* pp. 1-12, 2014.

[38] J. Scruggs, I. Cassidy and S. Behrens, "Multi-objective optimal control of vibratory energy harvesting systems," *Journal of Intelligent Material Systems and Structures,* pp. 2077-2093, 2012.

[39] W. Zhou and L. Zuo, "A self-powered piezoelectric vibration control system with switch precharged inductor (SPCI) method," *ASME Transactions on Mechatronics,* pp. 773-781, 2015.

[40] S. Sharuz, "Limits of performance of mechanical band-pass filters used in energy scavenging," *Journal of Sound and Vibration,* pp. 449-461, 2006.

[41] E. Leland and P. Wright, "Resonance tuning of piezoelectric vibration energy scavenging generators using compressive axial preload," *Journal of Smart Materials and Structures,* pp. 1413-1420, 2006.

[42] C. Lu, C.-Y. Tsui and W.-H. Ki, "Vibration energy scavenging system with maximum power tracking for micropower applications," *IEEE Transactions on Very Large Scale Integration (VLSI) Systems,* pp.

2109-2119, 2011.

[43] D. Benasciutti, L. Moro and S. Zelenka, "Vibration energy scavenging via piezoelectric bimorphs of optimized shapes," *Microsystem Technologies,* pp. 657-668, 2010.

[44] E. Sardini and M. Serpelloni, "An efficient electromagnetic power harvesting device for low-frequency applications," *Sensors and Actuators A: Physical,* pp. 475-482, 2011.

[45] R. McMillan, *RE: No Power Strike - Amount of Power Required,* Cambridge: Email Correspondence, 2014.